Nanostructured Photocatalysts for Degradation of Environmental Pollutants

Shafali, Surinder Singh, and Sushil Kumar Kansal

Abstract Water is the most essential life form on earth and a prerequisite for human survival. Due to manifold anthropogenic and industrial activities, voluminous discharge of diverse organic and inorganic pollutants has blown up into the water bodies. Organic pollutants, in particular, have a major contribution to the degradation of water quality on a vast scale. There is an exigent need for the abatement of these organic contaminants from water and wastewater. There are many conventional techniques of wastewater treatment including sedimentation, filtration, adsorption, reverse osmosis, ion exchange, coagulation and flocculation, and Fenton process. Photocatalysis is a highly efficient technique for the degradation of organic contaminants from water and wastewater. Several semiconducting materials have been used as photocatalysts, including ZnO, WO_3, TiO_2, Fe_2O_3, and ZnS, for the photocatalytic decomposition of multifarious organic pollutants. These semiconducting materials are highly beneficial for their application in the photocatalytic treatment of wastewater due to their favorable properties. They have favorable electronic structure, excellent charge transfer properties, a long lifetime in the excited state, high stability, low cost, and strong capability to absorb light. However, due to the wide gap, their application is limited to ultraviolet region with only 5% of the total spectrum of available solar light. So, modified metal oxide-based photocatalysts have been employed for the effective utilization of a wide visible spectrum of light. To modify and enhance the efficacy of these catalysts, various methodologies such as nano-structuring, metal doping, and genesis of nanocomposites have been engineered. These modified nanostructured photocatalysts provide an effective treatment potential to degrade organic water pollutants. This chapter outlines the potential and efficacy of metal oxide and modified metal oxide-based photocatalysts for the treatment of contaminants from water and wastewater.

Keywords Metal oxide · Organic pollutants · Photocatalysis · Modified metal oxide-based photocatalysts

Shafali · S. Singh (✉) · S. K. Kansal
Dr. S. S. Bhatnagar University Institute of Chemical Engineering and Technology, Panjab University, Chandigarh, India

K. K. Pant et al. (eds.), *Catalysis for Clean Energy and Environmental Sustainability*, https://doi.org/10.1007/978-3-030-65017-9_26

1 Introduction

Water happens to be the most vital and essential natural commodity for the survival of different forms of life on earth. However, providing access to clean and safe drinking water for everyone has become a daunting task globally [1, 2]. According to an annual report by WHO published in 2018, around two billion people were forced to consume water that is contaminated with fecal material, while 4.5 billion had access to poor sanitation systems [3]. It is estimated by the United Nations that around 1.7 million or nearly 3.1% of worldwide deaths every year are due to the consumption of contaminated water [4]. Globally, more than one-fifth of children die from water-related diseases such as diarrhea under 5 years of age, and about 4500 children get demised every day due to diarrhea [5]. The scarcity of safe drinking water is attributed to the competing and selfish needs of the rapidly growing population which have been overrun by water supplies. It is expected that this issue will become even more serious as the population increases by around two billion by the year 2050 [6]. Besides the increasing population, the rapid release of harmful chemicals by industrialization and anthropogenic activities into the water also have an equal contribution to the scarcity of water. On average, about two million tons of waste including agricultural, sewage, and industrial waste is released into water bodies daily [7, 8]. This dumping of waste leads to the introduction of inorganic, organic, radioactive, and biological pollutants into the water bodies and causes a massive deterioration in the quality of water. Among all these pollutants, organic pollutants, in particular, pose a serious threat to society because they have been widely used in textile, agricultural, and pharmaceutical and other chemical industries. Various types of organic pollutants, such as polychlorinated biphenyls (PCBs), dyes, phenolic compounds, pharmaceutical drugs, cosmetics, polycyclic aromatic hydrocarbons (PAHs), pesticides, and herbicides, have detrimental effects on human health such as cancer, disturbance in the endocrine system, obesity, and reproductive system disorders [9–12]. The effects of these pollutants are not just limited to human health, but entire ecosystems have been disrupted by these pollutants. Marine life, in particular, has been the worst affected with around 50% of the fish species and one-third of the amphibian population reportedly extinct [13]. The removal of organic contaminants from water/wastewater is necessary because of their consistent and tremendously increasing occurrence in water in the present time. They are ubiquitous due to their semi-volatility, meager hydrophilicity, toxicity, bioaccumulation, and non-biodegradability under ambient conditions [12, 14]. Due to the detrimental effects of organic pollutants on all living organisms and the environment, it becomes necessary to remove them from water/wastewater so that the treated water can be efficiently reused for the world's sustainable and economic growth. The problem of shortage of water can be overcome by developing suitable methods and materials which are economic, reliable, and efficient and that can meet the high environmental standards. The conventional water purification techniques like flocculation, activated sludge, biological trickling filters, chlorination, ozonation, filtration, precipitation, sedimentation, coagulation, adsorption, oxidation, distillation,

reverse osmosis, etc. had been employed to remove organic pollutants from water/wastewater, but these methods have some limitations also. These techniques are not sufficient individually to remove a wide spectrum of organic pollutants since most of them are not capable to remove microbes that cause diseases like cholera, typhoid, etc. Also, some of these techniques can only transform the phase of the pollutants and/or lead to the generation of secondary pollution that needs further treatment [15, 16]. Recently, semiconductor photocatalysis has emerged as the most effective technique for the degradation of organic impurities from water/wastewater. This technique is simple, is economical, and can completely mineralize the organic contaminants to non-toxic compounds such as CO_2 and H_2O without the formation of secondary pollutants. The most important and unique features of photocatalysis are usage of solar irradiation, the most abundant source of light, and its conversion into chemical energy for its use for the treatment of water contaminants [17–19]. Several semiconducting materials had been utilized for photocatalytic decomposition of organic impurities. Among them, metal oxides such as TiO_2, ZnS, and ZnO are the most widely used traditional heterogeneous photocatalysts for organic wastewater treatment. They have excellent properties such as good stability, an efficient capability to absorb light, complimentary electronic structure, charge transfer properties, and lifetime in the excited state. However, these catalysts suffer from one major limitation that they have a wide bandgap, so they can utilize the ultraviolet region of electromagnetic spectrum only [20–27]. Since metal oxides have some inherent limitations, physical or chemical modifications in their structure are required to enhance their photocatalytic activity. These modifications or changes in metal oxide catalysts include imparting nanostructure to these materials, doping, and formation of composites with other materials [28–30]. Nanostructure engineering involves reducing the size of the catalyst to a nanoscale, which ultimately changes the material properties tremendously. One major advantage of both the nanostructured materials is excellent recyclability and the ability to regenerate for several cycles [31, 32]. Similarly, the formation of composites and doping methods have also been reported to enhance some properties such as to broaden the light absorption spectrum, reduced recombination of charge carriers, reduced bandgap energy, and high specific surface area [33–36]. Although photocatalysis has emerged as an economical and environmentally friendly sustainable technology, it is yet to fulfill the requirements of the industry. The development of a perfect photocatalyst possessing outstanding photocatalytic efficiency, large surface area, the ability to completely utilize sunlight, and superior recyclability remains, by far, the biggest challenge on the path to its commercialization.

The current chapter aims to describe the overview about the most basic principles of photocatalysis and the role and application of traditional photocatalysts such as metal oxide catalysts in the removal of harmful organic contaminants from water. This chapter also includes discussion on methods to enhance photocatalytic efficiencies such as nanostructure engineering, the addition of external materials or doping, and the formation of composites, and finally, the chapter concludes with potential prospects in the area of photocatalysis.

2 Scope of Photocatalysis for the Degradation of Organic Pollutants

The removal of toxic, burgeoning, and recalcitrant organic pollutants from water has now become an imperative task. Organic pollutants are the pollutants that have the potential to persist for a prolonged time, are produced extensively by industries, have high stability at ambient temperatures and in sunlight, and have a strong resistance to degradation. They have great adverse implications on the human and animal's health, aquatic species, other living beings, and the environment. They can cause cancer, reproductive system disorder, and disturbance in the immune system, affect the growth of children, and cause mutagenic and carcinogenic effects on human health [12, 14, 37]. As a result, the immediate development of an ideal and most reliable treatment method has become an essential need for society at present. To date, many physico-chemical and biological techniques have been explored for the decomposition of organic pollutants from water/wastewater as shown in Fig. 1.

The most commonly used methods are coagulation-flocculation, activated sludge process, membrane process, ozonation, biological treatment, filtration, reverse osmosis, ion exchange, Fenton process, adsorption, and photocatalysis [15, 16]. However, the coagulation-flocculation process is only effective in removing turbidity and color and is unable to remove organic/inorganic pollutants, dissolved impurities, and heavy metals [38]. The activated sludge process has its own sets of limitations such as the formation of loose flocs, high operating costs, sludge expansion, and poor effluent quality [39]. The ozonation process is often used for water disinfection, but it leads to the formation of carcinogenic bromates as byproducts in the treated water and is also an expensive process [40]. Biological treatment is not

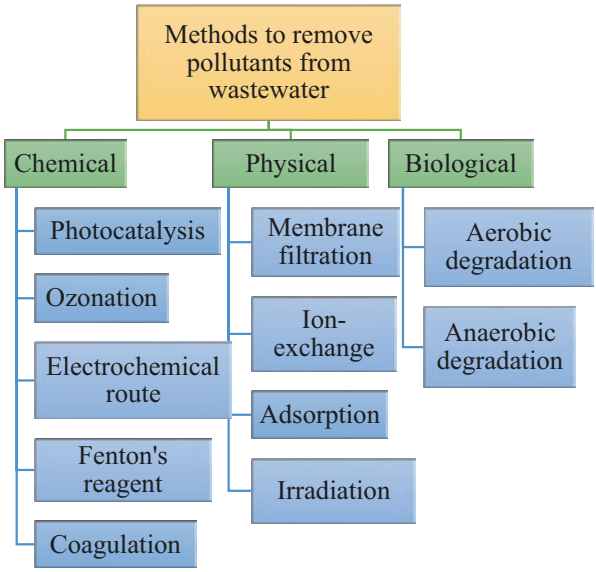

Fig. 1 Methods to remove pollutants from water/wastewater

effective in eliminating high concentration pollutants, requires a high level of oxygen and qualified operators, and is unable to remove certain organic pollutants that are resistant to biological degradation [41]. The filtration process can efficiently remove pathogens and turbidity adequately, but has poor response towards the removal of organic materials and also causes the formation of excess amount of disinfection byproducts when chemical disinfectants are added [42]. Membrane processes such as reverse osmosis suffer from the limitation of clogging of pores by the pollutants which makes them inefficient in removing contaminates after a short time. They also produce fouling odor caused by the scaling of colloidal, particulate, organic, and biological pollutants [40]. In the ion-exchange method, the majority of the resins get polluted in the presence of organic materials [43]. The Fenton process produces iron sludge that causes secondary pollution, is an expensive process, requires a narrow working pH range, and includes risks of handling, storage, and transportation of reagents [44]. The adsorption technique is the most widely employed and efficient method for wastewater treatment, but this process has also some major drawbacks like high cost, small capacity, and unsuitable for large-scale applications [45]. Moreover, all these abovementioned methods are not easy to use, i.e., need additional equipments/resins, and are not economic and environmentally friendly as they are only capable of transferring the phase of pollutants from one phase to another. These methods may also produce secondary pollutants that need further treatment and therefore increase the cost of the treatment process [15, 16]. Therefore, we need a method that can meet the essential requirements such as environmentally benign, have a low cost, capable to completely mineralize the parent as well as intermediate pollutants, flexible, highly efficient, and possessing high recycling capacity. Until now, semiconductor-based photocatalysis played an important part in the advanced oxidation processes (AOPs). It is the most reliable and promising approach that can meet all the abovementioned requirements for the decontamination of organic pollutants from water/wastewater [15–19]. The number of publications on environmental remediation using photocatalysis technique has increased productively over the last 16 years. The number of publications was found to have increased ten times in 2002 as compared to 2001, and more than 6000 publications were published during 2017 [46]. Also, the number of publications on photocatalysis displayed a significant increase from 2000 to 2019 as shown in Fig. 2 [47].

2.1 Photocatalysis

It is defined as the chemical reaction involving a catalyst which accelerates the reaction rate, utilizing the solar spectrum. The phenomenon of photocatalysis was initially discovered by the scientists Fujishima and Honda in 1972 during their experiment on splitting of water on TiO_2 electrode [48]. Since then, extensive study and research have been carried out by the scientists for understanding the basic mechanism and parameters affecting photocatalysis so that this technique may be

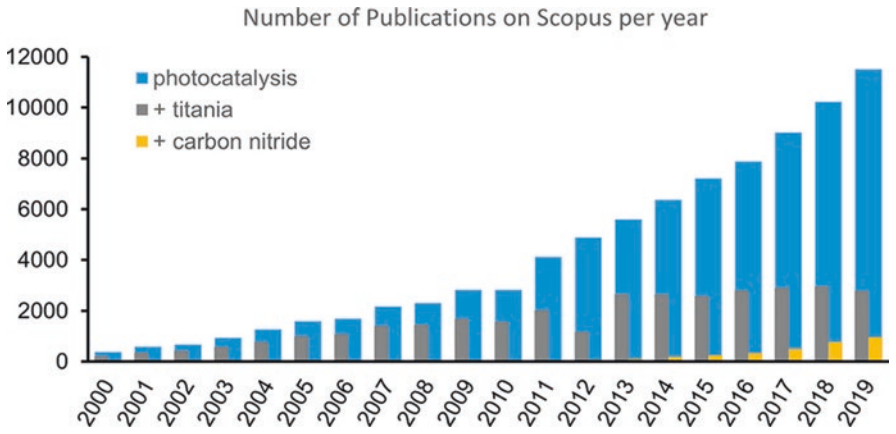

Fig. 2 Histogram of the number of publications on photocatalysis (blue bars) and on photocatalysis with TiO_2 and C_3N_4 (gray and yellow bars, respectively) from 2000 to 2019 (Data source: Scopus March 12, 2020) (Reproduced from Melchionna et al. 2020 [47])

applied to water/wastewater treatment applications. Photocatalysis technique can be categorized into two categories: (1) homogeneous and (2) heterogeneous photocatalysis. During the process of homogeneous photocatalysis, all reagents and photocatalysts are present in the same phase. Commonly utilized catalysts in this process are transition metal complexes, e.g., iron, chromium, and copper. However, during heterogeneous photocatalysis, all reagents and photocatalysts tend to present in different phases. The process includes semiconducting materials like TiO_2, ZnO, SnO_2, etc. However, due to the outstanding properties of the semiconducting materials used in the latter process, it has gained huge attention compared to the former. These materials have exceptional properties such as suitable electronic structure, excellent stability, high absorption coefficients, high ability to generate charge carriers when the light of suitable energy falls on them, biocompatibility, high charge transfer properties, and excited lifetimes of metal oxides. Also, heterogeneous photocatalysis proves to be highly efficient in degrading distinct organic impurities to biodegradable intermediates and also mineralizing them completely to non-toxic carbon dioxide and water molecules by undergoing a suitable photocatalytic mechanism [49–51].

2.1.1 Mechanism of Heterogeneous Photocatalysis

Heterogeneous photocatalytic mechanism incorporates the following basic steps:

1. The electrons from the valence band (VB) of the semiconductor material get transferred to the conduction band (CB) when the light of suitable energy (i.e., equal to or more than the bandgap energy) is incident on the surface of semiconductor.

2. Holes that are generated in valence band (VB) after the transfer of electrons participate in the oxidation of donor molecules and generate hydroxyl (OH·) radicals after reaction with water.
3. The electrons in the conduction band (CB) can react with species of the dissolved oxygen to form superoxide ions. Redox reactions are induced by these electrons followed by successive reduction and oxidation reactions that occur between any species that might have been adsorbed on semiconductor surface. The mechanism of semiconductor photocatalysis is shown by the following schematic, i.e., in Fig. 3.

The formation of radicals is initiated by a series of steps as shown below:

- $TiO_2 + hv \rightarrow e^{-}$(conduction band) + h^{+}(valence band.).
- $O_2 + e^{-} \rightarrow {}^{\cdot}O_2^{-}$.
- ${}^{\cdot}O_2^{-} + H_2O \rightarrow HO_2^{\cdot}$.
- $H_2O/OH^{-} + h^{+} \rightarrow HO^{\cdot}$.
- $\cdot O_2^{-} / \cdot O_2H / OH\cdot + \text{organic pollutants} \rightarrow CO_2 + H_2O$.

The generated $OH^{\cdot}$ and $\cdot O_2^{-}$ ions play a major role to degrade organic pollutants. Firstly, the pollutants are transferred from the bulk liquid phase (BLP) to the surface of catalyst. Secondly, the surface of the photon-activated photocatalyst is used for adsorbing the impurities on its surface, followed by generation of $OH^{\cdot}$ and $\cdot O_2^{-}$ radicals which will further degrade the impurities to non-toxic mineralized products, e.g., CO_2 and H_2O. Finally, the intermediates or the final products formed during the

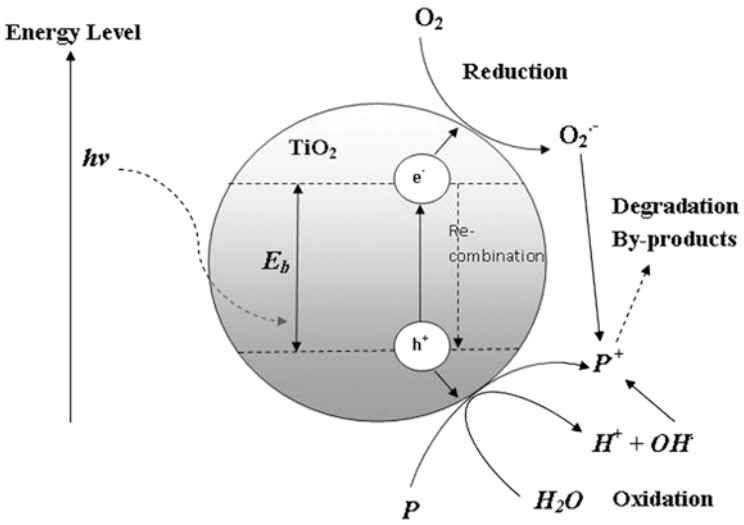

Fig. 3 Photo-induced formation mechanism of electron-hole pair in a semiconductor TiO_2 particle with the presence of water pollutant (P) (Reproduced from Chong et al. 2010 [54])

reaction are desorbed from the catalyst surface and transferred to the bulk liquid phase (BLP) [52–54].

Various catalysts had been discussed in literature by researchers for the degradation of organic contaminants, but only a few of them, which are highly efficient due to their characteristic properties, e.g., metal oxides and their composites, will be discussed in the present chapter to fully understand the potential, applications, and merits of these photocatalytic materials in water/wastewater treatment.

3 Metal Oxide-Based Photocatalysts for the Treatment of Organic Pollutants

To date, a wide variety of photocatalysts have been reported for the treatment of organic species from water/wastewater. Photocatalysts are core of the photocatalysis technique; therefore, the design of an ideal photocatalyst is an essential task. An excellent photocatalyst is one that possesses a remarkable ability to harness visible or UV light coupled with high photocatalytic efficiency and stability towards photocorrosion. In addition to these properties, it also needs to possess biological and chemical inertness, has a low cost, and should be environmentally benign [55, 56]. During the last years, major research has been centered on semiconducting materials like metal oxides to treat wastewater possessing harmful organic impurities. Metal oxide photocatalysts like TiO_2, ZrO_2, ZnO, SnO_2, WO_3, Fe_2O_3, CeO_2, etc. have shown tremendous potential in photocatalysis due to their exceptional characteristics like diverse morphology, composition, structure, and size. Thanks to the electronic structure of these catalysts, due to which they can serve as sensors for light-induced redox processes, absorption of the light by semiconducting materials causes the charge transfer process due to the formation of holes that can oxidize the organic species [51, 57]. TiO_2 and ZnO are, by far, two of the most extensively studied metal oxide semiconducting materials [58–63]. Additionally, Fe_2O_3, SnO_2, and WO_3 are also the commonly used catalysts used for the treatment of organic impurities.

3.1 Discovery of TiO_2 as a Photocatalyst

TiO_2 is a metal oxide that occurs naturally and can be easily obtained from a mineral called ilmenite which is a titanium iron oxide mineral [64]. It can exist in three polymorphic forms: (a) anatase, (b) rutile, and (c) brookite [65]. Rutile happens to be the most commonly utilized and stable type of TiO_2 utilized at high temperatures; however, anatase form is only stable at low temperatures. Brookite form is in-between phase formed during anatase-to-rutile phase transformation. This form is metastable, is uncommon, and rarely exists [64, 65]. The ability of TiO_2 to exist and

to get converted in various physical forms such as powdered TiO_2, dispersed colloidal particles in water, thin films, nanoparticles, nanorods, etc. underlines their possible applications in TiO_2 photocatalytic technology [64].

The groundbreaking work of Fujishima and Honda initially unfolded titania (TiO_2)-based photocatalysis, sometimes quoted as "Honda-Fujishima effect." After that, numerous efforts to explore the photocatalytic properties of TiO_2 have been made. An early attempt on photocatalysis using an aqueous suspension of TiO_2 was initiated by scientists Frank and Bard during the year 1977 for the photo-oxidation of CN^- and SO_3^{2-} ions under sunlight [66]. A report displaying the ability of titania (TiO_2) to reduce CO_2 under visible light further drew the attraction of the researchers towards titania photocatalysts [67]. Since the 1980s, the photocatalytic decomposition of various harmful aqueous and air pollutants using powdered TiO_2 has become the subject of extensive research [68].

3.1.1 Photocatalytic Properties of TiO_2

TiO_2 basically is an n-type semiconductor material with an energy bandgap value ranging from 3.0 to 3.2 eV, the bandgap being low as compared to ZnO and tin oxide (SnO_2) which happens to be 3.35 eV and 3.6 eV, respectively (at about 400 nm wavelength). Thus, light having wavelength less than 400 nm will be required to initiate a photo-reaction using TiO_2 [69–71]. TiO_2, however, possesses remarkably high thermal and chemical stability coupled with its strong UV light absorption capacity that allows it to perform effectively in the degradation of organic pollutants. A strong oxidizing ability, high stability in any pH, hydrophilicity, environmental friendliness, ease of preparation, and high pigmentary properties are some of the other properties that make TiO_2 a great photocatalytic material [67–72]. The ability to yield results over a range of pH values is in stark comparison to ZnO, another widely used photocatalytic material, which can easily undergo corrosion in the acidic medium [72]. An important feature of TiO_2 is that the holes in the VB bear more oxidation potential as compared to electrons of CB. Also, the oxidation potential of VB holes is higher than the normal hydrogen electrode potential (NHE). Furthermore, the conduction band energy (CBE) possessed by TiO_2 catalyst remains higher than the reduction potential of oxygen, O_2 (a predominant electron acceptor), which induces electrons to move towards the conduction band to O_2 which results in the absolute mineralization of organic pollutants to H_2O and CO_2 [73]. Most of the photocatalytic chemical reactions involve water, air, pollutant, and photocatalyst. In terms of photocatalytic activity, anatase type of TiO_2 happens to be more efficient than rutile type because the former has an indirect bandgap as compared to the latter, which has a direct bandgap. As a result, anatase has a longer life, which drives the energetic separation of e^-/h^+ (electron-hole) pairs and inhibits the recombination [74, 75]. Also, position of CB of the anatase phase is such that it can drive more efficient conjugate reactions of electrons [76]. Other approaches, including the combination of rutile-type and anatase-type phases, have been employed to enhance the photocatalytic effect of TiO_2 as the e^-/h^+ recombination rate gets

declines in composite [77, 78]. As the edge of anatase CB is reported to exceed the rutile phase by a bandgap of 0.2 eV which makes the transfer of electrons smooth [79], this results in the jump of anatase electron to rutile phase, hence reducing e^-/h^+ recombination rates and evolution of holes on anatase site [80, 81]. Degussa type P25 TiO_2, containing 75% of anatase, and of 25% rutile part, is one such combination of the two phases of TiO_2 that is well known and has been commonly used commercial catalyst [77]. The photocatalytic efficiency of the TiO_2 greatly relates to charge carriers and surface densities of charge carriers. The e^-/h^+ pairs take a few femtoseconds (fs) to generate. Then within some picoseconds (ps) or nanoseconds (ns), charge carriers that have been induced by light can be trapped [82]. The electron and hole can be recombined in a few tens of nanoseconds [83].

Various TiO_2 photocatalysts got reported for studies related to decomposition of toxic organic pollutants present in aqueous medium. For example, TiO_2 Degussa P-25 was utilized in photodegradation of cationic dye malachite green (MG) under UV light. The as-prepared photocatalyst displayed 99.9% degradation of MG which was observed to decrease with decreasing pH. At low pH, the structure of MG dye got cleaved and so the dye adsorbed with difficulty at surface of the TiO_2, hence producing slow degradation efficiency. Under high pH, several intermediates were formed, and the dye got adsorbed at TiO_2 surface easily, the degradation rate being higher at high pH. Also, rate of degradation of MG dye was found to decrease with increasing catalyst concentration. This is because, at high concentrations of 0.5 g L^{-1}, less active sites got induced by aggregation of TiO_2 particles [84]. The influence of the pH value during photocatalytic treatment of MG using TiO_2 is displayed in Fig. 4.

The photocatalytic degradation of two dyes, i.e., acridine orange and ethidium bromide, under UV irradiation was also performed by using TiO_2 suspensions. It has been found that acridine orange was decomposed completely in 75 min, while ethidium bromide has undergone complete decomposition in 195 min. Further, the comparison of TiO_2 types like Degussa P25, Hombikat UV100, and PC500 was also

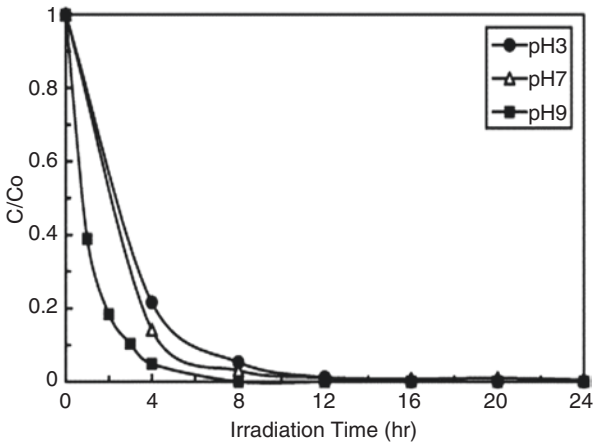

Fig. 4 pH effect on the MG photodegradation rate with concentrations of TiO_2 to be 0.5 g L^{-1} and MG to be 0.05 g L^{-1} (Reproduced from Chen et al. 2007 [84])

investigated. Degussa P25 was found to display maximum photocatalytic efficiency among the three types. Also, the photocatalytic capability enhanced with enhanced catalyst concentration, but after a particular concentration called optimum concentration, the reverse trend was observed, i.e., efficiency photocatalytic declined. This is because, beyond optimum concentration, the TiO_2 particles would start aggregating resulting in less active sites at surface of TiO_2 [85]. Yang et al. utilized Degussa P25 TiO_2 as a photocatalyst to degrade paracetamol utilizing UV light. Various important factors such as the effect of UV light, initial drug concentration, catalyst dose, pH, oxygen concentration in solution, and intensity of light were explored to determine the optimal set of conditions. Degradation of paracetamol utilizing UV A (365 nm) light was found to be negligible, while significant degradation was observed under UV C (254 nm) irradiation. The degradation rate enhanced with an increase in the intensity of light and oxygen concentration. Amount of drug degraded initially enhanced with an enhancement in catalyst dose but decreased when the loading was further increased. There was a slow rise in the drug degradation rate as the pH was raised from 3.5 to 9.5, and a further enhancement in solution pH beyond 9.5 led to a significant fall in degradation rate. Under the optimized conditions, more than 95% of the drug was degraded within 80 min [86]. Ohko et al. studied the photocatalytic treatment of bisphenol A employing commercially available anatase TiO_2 using UV irradiation. It was found that the adsorption isotherm of bisphenol A followed a Langmuir model and only 4% of the initial pollutant in the solution was adsorbed at surface of photocatalyst till 12 h. Nearly all of the bisphenol A present initially was degraded by the photocatalyst in a time period of 15 h, the degradation process being following the first-order-type kinetics. Another thing observed was the formation of intermediates during the early stages of photocatalytic degradation, and these intermediates were found to have been completely converted to CO_2 in 20 h under UV light irradiation [87].

3.2 ZnO and Its Advantages

ZnO has emerged as an equally good alternative to TiO_2 catalyst for treating organic impurities owing to its marvelous properties such as similar bandgap energy as that of TiO_2. Additionally, it is identical to TiO_2 in the dynamics of charge carriers upon excitation, as well as formation of the reactive oxygen atoms when suspended in the aqueous medium. The reasons behind its utilization as a photocatalyst include high photosensitivity, high redox potential, high thermal and mechanical stability, anisotropic growth, and ease of crystallization. Also, its low production costs, availability in nature in abundance, synthesis versatility with hierarchical morphology, and large bandgap make it hugely popular in photocatalysis [88].

The electron mobility of ZnO is in the range of 200–300 $cm^2\ V^{-1}\ s^{-1}$, and the lifetime of generated e^-(electron) is greater than 10 s. This makes ZnO having reduced electrical resistance, thus promoting the transfer of electrons with high speed [89, 90]. Also, the valence band possessed by ZnO is located below the valence

band of TiO_2, so hydroxyl radicals generated by ZnO will have enhanced oxidation potential (+3.06 V) when compared to TiO_2 (+2.7 V). While electrons generated from CB of ZnO are found to be more negative than TiO_2 (+2.7 V), the edges of CB of both the catalysts are believed to be located at the same position at the neutral condition of pH (−0.5 V vs. NHE) [91, 92]. Additionally, ZnO has high absorption efficiency over a broad spectrum of solar light than TiO_2. Fenoll et al. in their study investigated the photocatalytic effectiveness of ZnO and TiO_2 in degrading the fungicides in leaching water employing solar light [93]. Comparative study of both ZnO and TiO_2 for the treatment of cyprodinil and fludioxonil fungicides is shown in Fig. 5.

They found that the ZnO was more efficient than TiO_2 because of its non-stoichiometry. The photocatalytic activity was also examined for both ZnO catalyst and P25 TiO_2 catalyst for the treatment of acid brown 14. ZnO showed higher degradation when compared with TiO_2 due to the absorption of more quanta of light [94]. Also, the performance of ZnO catalyst was matched with TiO_2 for photocatalytic degradation of terephthalic acid (TPA) from wastewater using UV light. The degradation rate of TPA using ZnO was much faster than utilizing P25 TiO_2 under optimized conditions [95]. Furthermore, the degradation efficiencies of ZnO catalyst and P25 TiO_2 catalyst were calculated to ascertain decomposition of estrone in aqueous medium using artificial ultraviolet (UVA) and solar irradiation. Under UVA irradiation, ZnO exhibited a three times more degradation rate as compared to P25 TiO_2, whereas under solar irradiation ZnO showed 2.7 times more degradation efficiency when compared to results obtained utilizing UVA irradiation [96]. ZnO was also found to be more capable than TiO_2 in degrading congo red azo dye [97]. Also, it was reported that ZnO displayed better photocatalytic activity for degrading the methylene blue (MB) dye than TiO_2 [98].

3.2.1 Significance of ZnO in the Efficient Removal of Organic Pollutants

The prominent feature of ZnO is that its photocatalytic reactions can be best performed at conditions of neutral pH. Furthermore, its emission properties render it to perform effectively in removing the pollutants from the environment [89, 99, 100], thus allowing the transfer of charge carriers generated by light to the surface in high concentration, which further contributes to the efficient removal of pollutants. Also, ZnO can absorb a significant fraction of quanta of light from a UV spectrum rendering it to perform better in wastewater treatment applications [101]. Moreover, ZnO scatters the light seldomly because of its smaller refractive index (RI = 2.0) as compared to TiO_2 catalyst (RI = 2.5–2.7), which results in boosting the transparency of ZnO [89]. The unique bending of the ZnO surface band in an upward direction in the air indicates that E (electric field strength) which is directed from the inner surface to the outer surface promotes the movement of electrons from the surface to the bulk. The holes move from the bulk to the surface, thus facilitating the adequate separation of e^- and holes [99]. Furthermore, immense binding energy of excitons (60 meV) and the defects like oxygen and zinc interstitials, vacancies, and hydroxyl and superoxide ions also enhance the photocatalytic capability of ZnO [101]. ZnO exhibits high photocatalytic capability than TiO_2 for treating organic impurities [93,

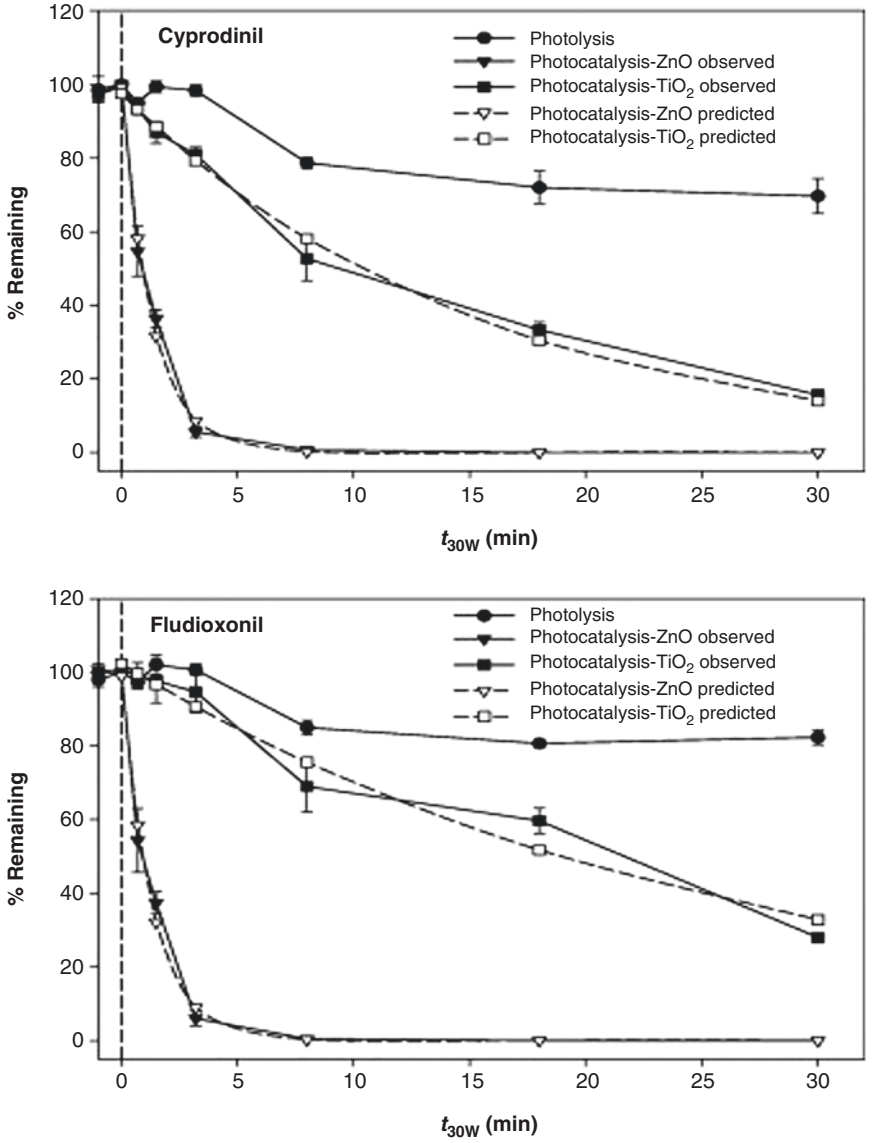

Fig. 5 Disappearance kinetics of cyprodinil and fludioxonil by photolysis (filled circle) and photocatalysis with ZnO (filled inverted triangle) and TiO_2 (filled square) during the photoperiod (as t_{30W}). Error bars denote standard deviation. Predicted kinetics according to a first-order model for photocatalysis experiments are shown, ZnO (triangle) and TiO_2 (square) (Reproduced from Fenoll et al. 2011 [93])

94, 102–106]. Degradation of insecticide diazinon from water under UV irradiation by using ZnO nanocrystals was also reported [107]. ZnO nanocrystals were synthesized by precipitation and calcination method, and maximum degradation rate was achieved with ZnO crystals of mean size of 14 nm. Around 80% of diazinon degraded within 80 min, and the degradation rate was excellent and more than the commercial ZnO catalyst. The enhanced photocatalytic efficiency of the prepared ZnO nanocrystals was due to the reduced size of nanocrystals from 33 to 14 nm [107]. El-Kemary et al. prepared nanostructured ZnO photocatalyst using chemical precipitation method for the treatment of ciprofloxacin (CF) using UV irradiation. The amount of drug degraded enhanced with enhancement in the solution pH in the range 4–10, with maximum degradation of 48% when the pH was 10. Higher degradation efficiencies under basic conditions were ascribed to the formation of hydroxyl ions which possess high oxidation capability. The degradation of drug followed the pseudo-first-order-type reaction kinetics [108]. The absorption spectra and the pseudo-first-order-type kinetics of CF are shown in Fig. 6.

The degradation of phenol was reported using commercially available ZnO under ultraviolet (UV), ultrasound (US), and a combination of UV and US irradiation. Sonophotocatalytic treatment of phenol was much more effective as compared to either photocatalytic or sonocatalytic degradation of the pollutant. Acidic pH and lower reaction volumes were observed to favor sonophotocatalytic degradation of phenol, with 85% of it getting degraded within 120 min. Phenol degradation process exhibited variable kinetics that depend on the pollutant concentration, and presence of anions such as chloride and sulfate could lead to a significant reduction in the amount of drug degraded [109]. ZnO photocatalysts bearing variable molar ratios of oxalic acid to zinc acetate precursors were prepared using sol-gel technique. The synthesized ZnO photocatalysts were explored for the treatment of dyes, e.g., congo red, direct black 38, and methyl orange, employing UV light from aqueous medium. ZnO sampled synthesized with precursor materials in the ratio 4:1 and further calcined at 400 °C exhibited high activity. Acidic conditions were determined to be the most favorable for the treatment of dyes; rates of removal of dyes were found to increase as the photocatalyst dose was increased and declined with enhancement of dye concentration. The photocatalyst was able to degrade 99.70% methyl orange, 97.53% congo red, and 89.59% of direct black 38 dyes in 30 min under UV light irradiation [110].

3.3 Other Metal Oxide Photocatalysts

3.3.1 Fe_2O_3

Recyclability is a very crucial aspect of the performance of photocatalyst. Recently, magnetic separation technology has emerged as the best alternative for the effective separation and recyclability of photocatalyst. Development of efficient catalysts having photocatalytic and magnetic properties has been the focus of researchers. In this context, Fe_2O_3 is being considered the most promising photocatalyst because of

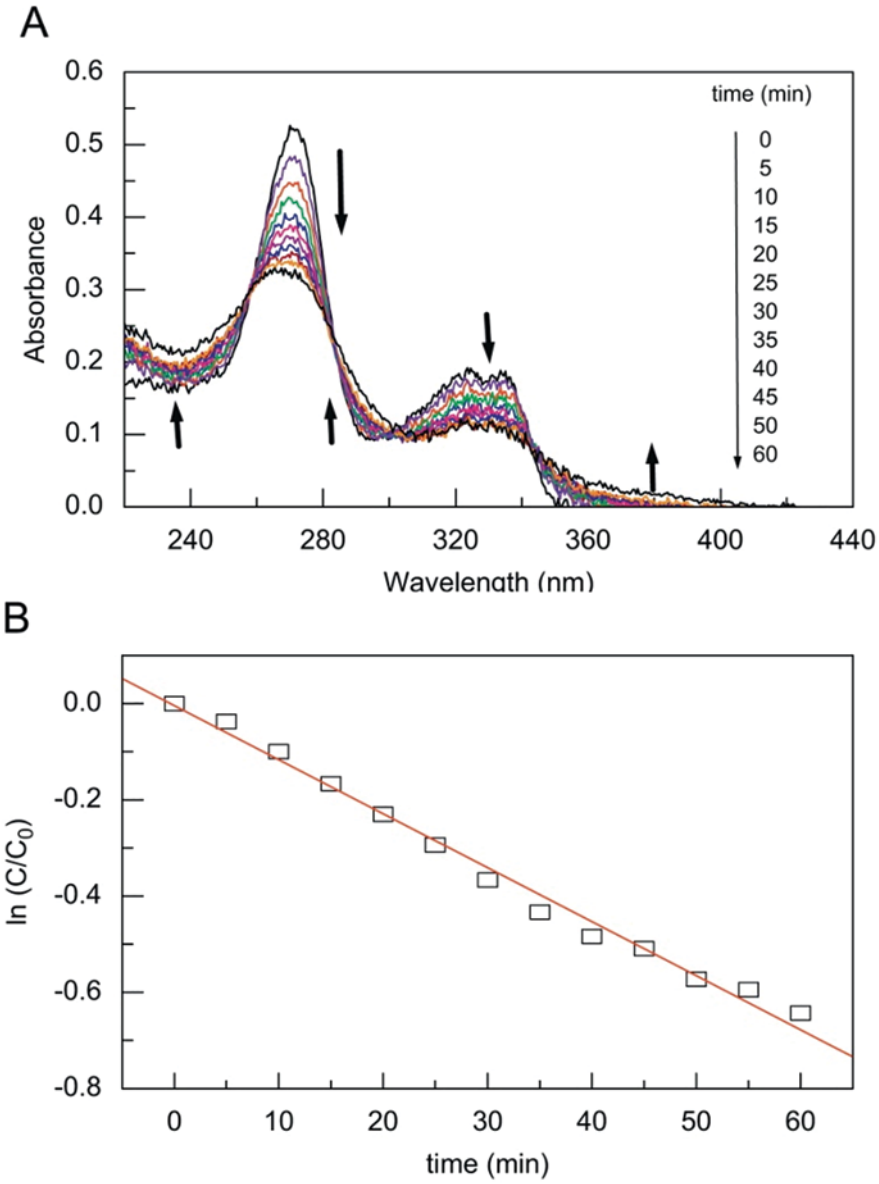

Fig. 6 (**a**) Change of absorption spectra of CF solution of pH 7 during photocatalytic degradation by ZnO nanoparticles and (**b**) pseudo-first-order plot for the kinetic photodegradation of CF in the presence of ZnO nanoparticles (Reproduced from El-Kemary et al. 2010 [108])

its favorable valence state and chemical composition, high resistance to corrosion, low toxicity, narrow bandgap energy (2.3 eV), excellent recyclability, natural availability in abundance, and high chemical stability. Additionally, it can harvest nearly 40% of the abundant solar light and has a saturated magnetization value of 1 emu g^{-1} which helps in the separation of photocatalyst via external magnetic field [111–114]. After absorption of light, generated e^- charge carrier species in Fe_2O_3 initiate chemical reactions through the activation of chemical compounds [115]. Fe_2O_3 catalyst plays a significant role in the separation of photocatalyst from solution and its degradation [116, 117]. Porous Fe_2O_3 nanorods were prepared by chemical solution technique and calcination. The as-synthesized catalyst was used for the photodegradation of methyl orange (MO), p-nitrophenol (pNP), rhodamine B (RhB), eosin B, and methylene blue (MB) utilizing solar light. The photocatalytic efficiency was found to be more efficient than the commercial Fe_2O_3 nanopowder degrading 87.2% of RhB in 180 min and 86.4% of eosin in 210 min. Other dyes were also degraded by Fe_2O_3 nanorods following an order of degradation as RhB > eosin B > MB > pNP > MO. The enhanced photocatalytic capability of prepared photocatalyst was by virtue of its porous nanostructure and larger specific surface area [115]. The photocatalytic degradation plot for RhB utilizing both the catalysts is shown in Fig. 7.

Use of UV laser was reported to be highly effective than conventional UV lamps, as in the study done by Gondal et al. In their work, α-Fe_2O_3 powder was employed for the photocatalytic degradation of phenol under UV laser irradiation. The results were estimated to be more efficient than those measured under conventional UV lamps. Photocatalytic degradation efficiency of phenol was recorded to be 90% in 1 h [118]. Shao et al. prepared ultrathin nanosheets of α-Fe_2O_3 using a dissolution-recrystallization method mediated by silica hydrogel. The prepared nanosheets were then explored using visible light photocatalytic degradation of bisphenol S. It was observed from the results of the study that the as-synthesized α-Fe_2O_3 nanosheets were able to remove 91% of bisphenol S present within 120 min under visible light illumination; by comparison, α-Fe_2O_3 nanoparticles and commercial TiO_2 were only able to degrade 16% and 62% within the same time period. Furthermore, rate constant for degradation of bisphenol S over α-Fe_2O_3 nanosheets was found to be 16.4 and 2.6 times greater than the rate constants obtained for degradation using α-Fe_2O_3 nanoparticles and commercial TiO_2, respectively. Similarly, the quantum efficiency of α-Fe_2O_3 nanosheets was found to be 4.5 and 1.9 times the quantum efficiencies of α-Fe_2O_3 nanoparticles and commercial TiO_2, respectively. The excellent performance of α-Fe_2O_3 nanosheets was attributed to the careful designing of the nanoarchitecture [119].

3.3.2 SnO_2

The structure of SnO_2 is the key to its effectiveness as a photocatalyst. Crystallographic structure of SnO_2 resembles rutile-type phase structure of titania TiO_2 [120]. The structural features of SnO_2 like the octahedral network are an essential prerequisite

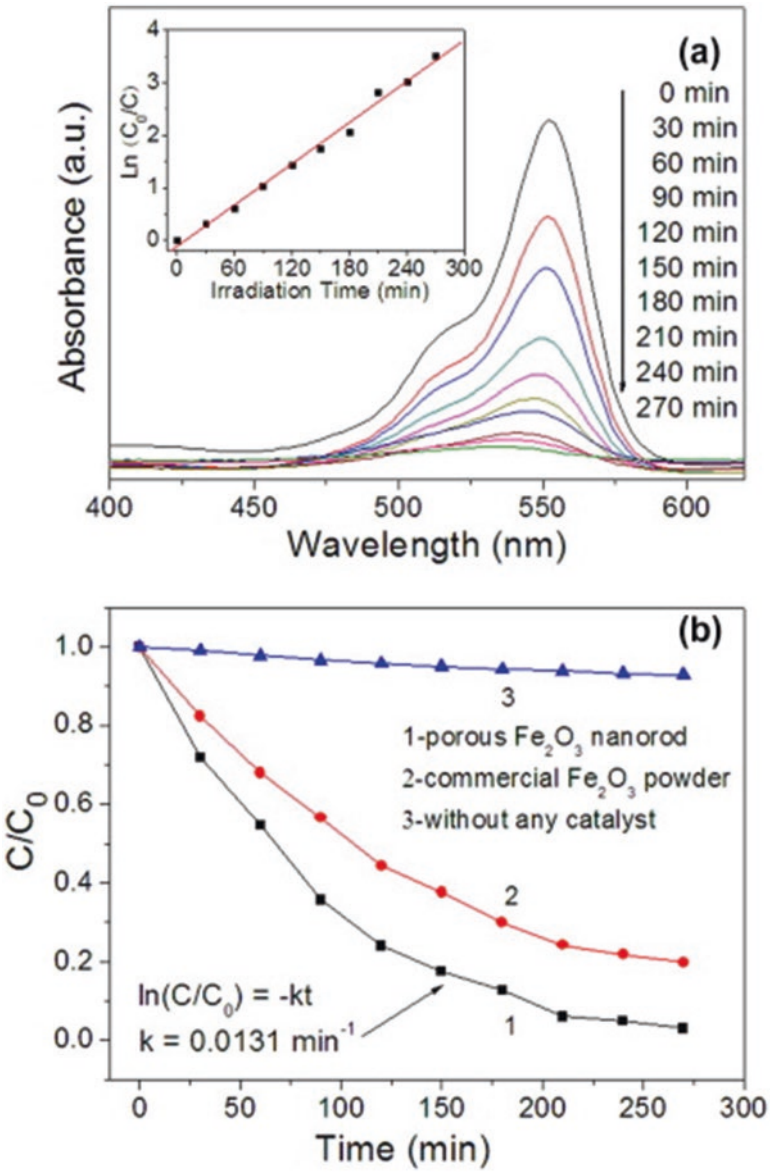

Fig. 7 (**a**) Changes in the absorbance spectra of the RhB in aqueous solution (10 mg/L, 50 mL) in the presence of porous Fe_2O_3 nanorods under the simulated solar light. (**b**) Photodegradation plots of RhB under the simulated solar light for different times in the presence/absence of the catalysts (Reproduced from Liu et al. 2015 [115])

for the high efficiency of photocatalyst as it helps in enabling increased mobility of electron-hole pairs, leading to the increase in probability of electron-hole pairs to reach the reactive sites on the photocatalyst surface [121, 122]. Some other essential properties of SnO_2 are high thermostability and photosensitivity, low cost and toxicity, low electrical resistance, high optical transparency, large bandgap, and high electrical conductivity owing to inherent structural defects [123, 124]. The presence of defects can lead to a significant decline in bandgap, thus enhancing the properties of SnO_2. In this context, more anions of oxygen cause oxidation of Sn from +2 to +4 state, to provide neutrality of SnO_2 [125, 126]. Due to the abovementioned properties, SnO_2 had been employed to treat toxic organic impurities from aqueous medium. Paramarta et al. described the synthesis of SnO_2 nanoparticles prepared using sol-gel technique for the removal of congo red (CR) and methylene blue under ultra-sonication and UV light. The photocatalytic activity was found to be greatly influenced by ultra-sonication irradiation. The sonocatalytic activity was estimated to possess a higher degradation rate, i.e., 48.5% for the dye congo red and 77.1% for the dye MB, as compared to a photocatalytic activity which displayed 32.6% and 64.1% for the dyes CR and MB [127]. Two-dimensional nanoflakes of SnO_2 were prepared employing hydrothermal technique for the sonophotocatalytic treatment of tetracycline hydrochloride utilizing visible light. The prepared nanoflakes of the photocatalyst displayed excellent photocatalytic activity towards tetracycline hydrochloride employing visible light. Furthermore, sonophotocatalytic process was much more efficient in degrading the drug as compared to photocatalysis or sonocatalysis; the sonophotocatalytic route was able to degrade nearly 89% of the drug present initially in 135 min utilizing visible light illumination. The degradation process exhibited pseudo-first-order-type kinetics; furthermore, the results of the scavenger study demonstrated that photo-induced holes along with superoxide radicals exhibited a major role in the sonophotocatalytic degradation of target drug [128]. Viet et al. used SnO_2 nanoparticles synthesized via hydrothermal route degradation of MB dye employing UV light irradiation. The synthesized nanoparticles of the photocatalyst were able to degrade nearly 89% of the initially present pollutant in 30 min utilizing UV light; degradation efficiency, thereafter, grew slowly and reached 90% after 120 min utilizing UV light. In comparison, commercial SnO_2 powder was able to degrade just 20.5% of the methylene blue initially present after 30 min of UV light illumination. When the same study was conducted under direct sunlight, synthesized SnO_2 nanoparticles were able to degrade 79.26% of the pollutant solution in 90 min, while the commercial SnO_2 nanoparticles degraded 36.23% of the pollutant solution in the same time period [129].

3.3.3 WO_3

WO_3 is an oxygen-deficient semiconductor that possesses bandgap energy varying from 2.4 to 2.8 eV. Its bandgap energy differs significantly with the defects or the stoichiometric ratio. It is photosensitive, is inexpensive, exhibits durable stability in various electrolytes, is non-toxic, and displays a higher light absorption coefficient

over a wide area of the solar spectrum (UV-visible). Additionally, it is resistant to photo decay, has a strong capability to convert the photoelectrons, is chemically inert, possesses high mechanical strength, and has long lifetimes of charge carriers [130]. Moreover, WO_3 can reduce charge carriers' recombination rate, exhibits a favorable rate of oxidation, and displays excellent efficiency to absorb light. It is capable of utilizing about 30% of abundantly present solar light. Furthermore, the valence and conduction band positions of WO_3 are favorable to degrade the organic pollutants, and, also, it is efficient to degrade acidic organic compounds because it can persist in the acidic climate for a prolonged time [64]. Three-dimensional WO_3 octahedra were prepared using simple hydrothermal technique for the photocatalytic degradation of MB dye employing visible light. The synthesized sample displayed higher degradation efficiencies as its dose in the pollutant solution was increased, with a photocatalyst dose of 100 mg degrading 95% of the initially present methylene blue in just 60 min. The degradation of MB dye followed pseudo-first-order-type reaction kinetics. Furthermore, it was observed that the WO_3 octahedra displayed a photocatalytic activity that was about 5.33 times more than bulk WO_3; higher photocatalytic activity of synthesized WO_3 octahedra was attributed to good crystallinity, high surface area, sufficient bandgap value, and more catalytically active sites [131]. Huang et al. employed simple hydrothermal route to synthesize nanoplates and hierarchical flower-like assemblies of WO_3 for the treatment of rhodamine B (RhB) dye utilizing the visible light illumination. The nanoplates and flower-like assemblies displayed degradation rates that were 7.6 and 3.3 greater than those of commercial WO_3 particles. The best photocatalytic activity was demonstrated by the nanoplates which were able to degrade almost all of the rhodamine-B after 150 min of visible light illumination [132]. The rate of degradation of rhodamine B using different morphologies of WO_3 photocatalyst is displayed in Fig. 8.

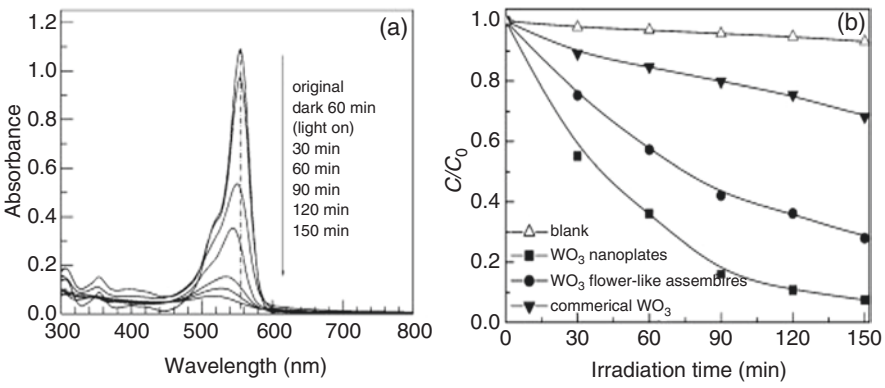

Fig. 8 (**a**) UV-Vis spectral changes of RhB aqueous solution in the presence of WO_3 nanoplates under visible light irradiation; (**b**) degradation rate of RhB over different photocatalysts (Reproduced from Huang et al. 2013 [132])

A hydrothermal route was employed to synthesize WO_3 photocatalyst for treating amoxicillin employing simulated sunlight. The study was conducted by making use of Box-Behnken design with initial concentration (of drug), catalyst dose, and solution pH as the independent variables and involving 30 experimental runs. It was observed from the study that while the amount of drug degraded enhanced as the catalyst dose was enhanced, it decreased as the solution pH and initial concentration of the drug both increased. The photocatalyst WO_3 was able to complete degrade amoxicillin in 180 min of simulated solar light illumination; however, the dissolved organic carbon (DOC) removal rate is only 36% in the same time period, which indicates the incomplete mineralization of the intermediates which were formed in the degradation process. The degradation process was found to follow pseudo-first-order kinetics; experimental data was best described using second-order polynomial regression models [133].

3.4 Strategies to Improve the Photocatalytic Efficiency of Metal Oxide-Based Catalysts

Over the years, metal oxide catalysts have been considered to be potential photo-induced catalytic materials due to their excellent properties. They have generally provided good results for the treatment of organic impurities found in wastewater. Still, their industrial applications have so far been limited due to factors such as e^-/h^+ pair recombination, lower quantum yield, and lower photocatalytic performances. Also, they are unable to utilize the full spectrum of sunlight due to their wide band-gap energies that allow them to use only the highly energetic UV region, which makes up only about 5% of the solar light spectrum. Recently, a series of strategies have been employed to make efficient use of these photocatalysts like nanostructure engineering, doping, and formation of composites [28–36].

3.4.1 Nanostructure Engineering

Nanostructure engineering involves the synthesis of nanostructured materials, which will change or manipulate the properties and functionalities of the photocatalytic materials at the nanoscale. The conversion of macro- and microstructures to nanoscale by nanostructure engineering has broadened the applications of photocatalysts. Recently, nanostructured metal oxides possessing enhanced photocatalytic properties have drawn the attention of researchers. Nanostructured metal oxides (NMOs) have been reported to possess optical, mechanical, electronic, and magnetic properties that do not exist in the bulk forms. Additionally, NMOs have also been reported to possess large surface area-to-volume ratios and small sizes than bulk materials, which result in increased photocatalytic activities [134, 135]. For instance, nanosized TiO_2 is reported to have a higher rate of photo-conversion

of organic compounds to mineralized products [136, 137]. Also, TiO_2 nanotubes displayed high photocatalytic efficiency as compared to available commercial TiO_2 (P-25 TiO_2) [138]. Furthermore, crystalline TiO_2 nanoparticles synthesized in our lab displayed superior photocatalytic performance for the degradation of Eriochrome Black T (EBT). The as-synthesized TiO_2 nanoparticles displayed higher degradation rate than commercially available PC-50, PC-500, and ZnO [139]. Nanostructured ZnO nanomaterials also exhibit better photocatalytic performance than pure ZnO, e.g., nanostar ZnO showed enhanced mass transfer of hydroxyl radicals during the photochemical reaction of methyl orange degradation [140]. The SEM images of nanostar ZnO photocatalyst at different reaction times are displayed in Fig. 9.

Also, ZnO nanoparticles synthesized by facile hydrothermal process displayed enhanced photocatalytic performance to degrade Alizarin Red S dye than commercial PC-500 photocatalyst [141]. Furthermore, porous Fe_2O_3 nanorods were synthesized and displayed more efficient photocatalytic efficiency, superior reusability, and stability than commercial Fe_2O_3 powder [116]. In another study, Fe_2O_3 nanowires were used for RhB degradation which also displayed better photocatalytic performance [142]. SnO_2 nanocrystals also resulted in the 100% degradation of RhB [143]. The enhancement in the photocatalytic efficiency of the abovementioned studies was due to the increased surface area, decreased distance of electron-hole transmission, and decreased electron-hole recombination rate.

3.4.2 Doping

Doping is considered to be the most promising, effective, facile, and practical approach to enhance photocatalytic properties because it can reduce the bandgap values of metal oxides, lead to enhanced charge separation, and result in shift in the absorption band to visible region. Also, this method leads to a change in the coordination environment of the host metal ion in the lattice. It introduces localized energy levels in bandgap states, which will modify the electronic band structure. The dopant can be introduced into the semiconducting materials either individually or

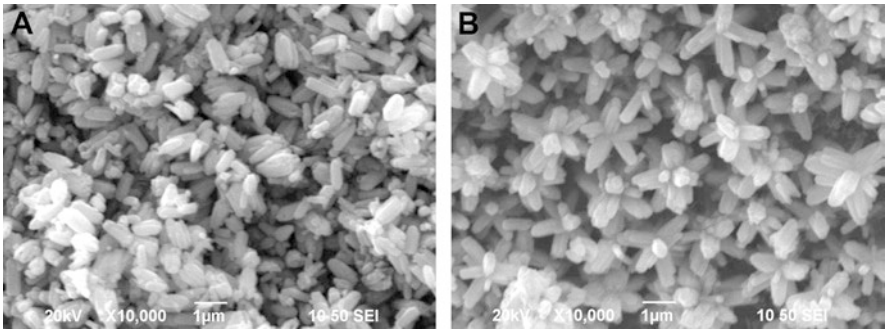

Fig. 9 SEM images of the ZnO products taken at different reaction times: 0.5 h (**a**) and 16 h (**b**) (Reproduced from Fang et al. 2013 [140])

simultaneously. Over the years, various metals, metalloids, and nonmetals have been used as dopants to increase the performance of metal oxide photocatalysts with excellent results [144–150]. For instance, doping of 13.36% Se on TiO_2 displayed outstanding photocatalytic capability employing visible light due to the narrowing of bandgap [151]. Also, N-doped Ti_4O_7 exhibited marvelous photocatalytic activity degrading 100% dye due to a reduction in bandgap energy from 2.9 to 2.7 eV of Ti_4O_7 [152]. Bimetallic-doped TiO_2 displayed more efficient results than single-doped TiO_2, e.g., the absorption band of Er-W-co-doped TiO_2 shifted to the near-IR range (800–1000 nm) [153]. The effect of doping various species on degradation efficiency of TiO_2 is displayed in Fig. 10.

ZnO has also been found to be affected significantly by the doping species, e.g., Pd^{2+}-doped ZnO displayed more efficient results towards the treatment of methyl orange (MO) dye. The incorporation of Pd^{2+} ions gave rise to electronic energy level in bandgap states, which helps in the trapping of charge species carriers. And the charge was efficiently separated with an increase in Pd^{2+} content from 2% to 3%, followed by a sudden decrease at high concentration [154]. ZnO plates doped with Ag ions have been used for the degradation of ofloxacin drug under solar irradiation. The as-prepared photocatalyst displayed enhanced degradation rate with 98% removal of ofloxacin in 150 min. The enhanced degradation rate was due to the trapping of electrons by silver ions which inhibited recombination of e^-/h^+ pairs [155]. Also, nitrogen-doped ZnO showed visible light photoactivity towards the degradation of bisphenol A due to the formation of isolated nitrogen 2p states above the valence band, which intensifies the visible light absorption [156]. Similarly, Pt-doped Fe_2O_3 showed a significant increase in the performance because Pt plays the role of conduction band electron sinker owing to its lower Fermi level, which

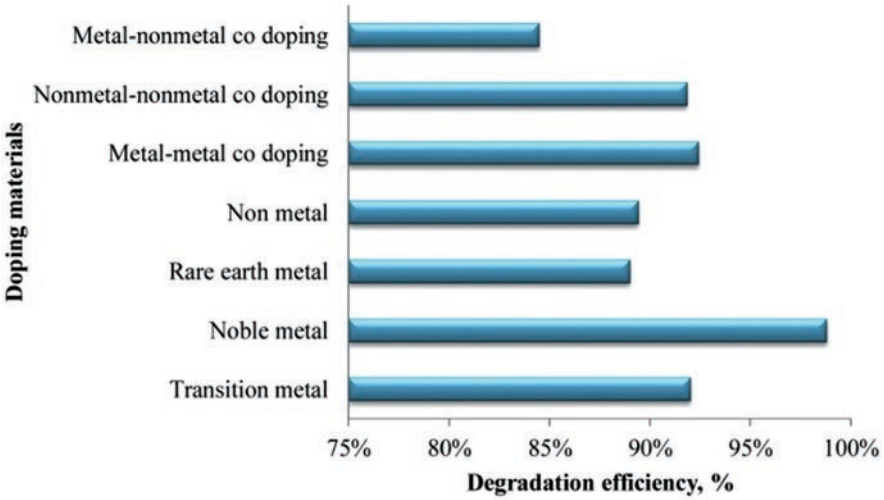

Fig. 10 Diagram for average photocatalytic degradation of different doping materials by using TiO_2 photocatalyst in the presence of UV irradiation (Reproduced from Al-Mamun et al. 2019 [73])

Table 1 Doped metal oxides that have been used for the degradation of organic pollutants from water

Pollutant	Photocatalyst	Synthesis method	Light source	Degradation efficiency (%)	Reference
Eosin yellow	Pd-/N-doped TiO_2	Nebulized-pray pyrolysis	UV irradiation	99.3	[158]
Congo red	Cu-/Zn-doped TiO_2	Sol-gel	Visible irradiation	98	[159]
Methylene blue	C-/F-doped TiO_2	Hydrothermal	300 W Xe lamp	75	[160]
P-nitrophenol	(a) Li-doped ZnO (b) Na-doped ZnO (c) K-doped ZnO	Sol-gel	Visible irradiation	Li-ZnO = 97 Na-ZnO = 72 K-ZnO = 84	[161]
Methyl orange	Au-doped ZnO	Hydrothermal	300 W Xe lamp	100	[162]
Methylene blue	ZnO-doped SnO_2 nanoparticles	Hydrothermal	UV irradiation	75	[163]
Formaldehyde	N-doped ZnO	Calcination	1000 W Xe lamp	97	[164]
Methylene blue	CdO-doped ZnO	Electrospinning	Sunlight irradiation	100	[165]
Phenol	Ce-doped ZnO	Chemical precipitation	Visible irradiation	80.7	[166]

improves the separation of electron-hole pairs [150]. Similarly, a considerable improvement was observed in Sb-doped SnO_2 due to the improved electrical conductivity of SnO_2 and modification in its band structure. This is because Sb traps the e^-/h^+ pairs and causes effective charge separation in the catalyst [157]. Some other examples of doped metal oxides are displayed in Table 1.

3.4.3 Formation of Composites

Formation of different composites/heterojunctions has drawn the utmost attention in recent years because of their facile synthesis, stability, and outstanding performance in the visible/solar light region. A heterojunction comprises two or more semiconducting materials, with one of them having a wide bandgap and the other having a narrow bandgap. While wide bandgap semiconductors such as TiO_2 are unable to absorb visible light, the narrow bandgap semiconductors, despite their ability to utilize the broad spectrum of light, suffer from the limitation of recombination of charge carriers. The formation of heterojunction results in the shifting of the absorption region beyond the UV region and also improves the separation of e^-/h^+ pairs [72, 167]. Therefore, the formation of heterojunction is necessary to explore

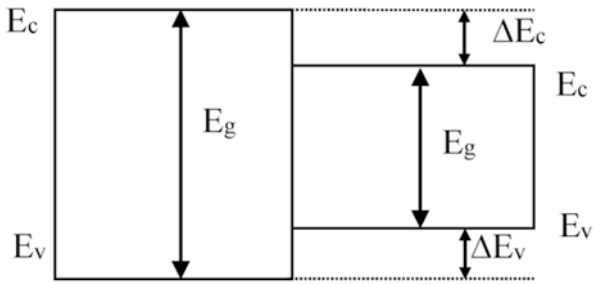

Fig. 11 Type I heterojunction with redox potential energy of CB (Ec) and VB (Ev) (Reproduced from Ani et al. 2018 [72])

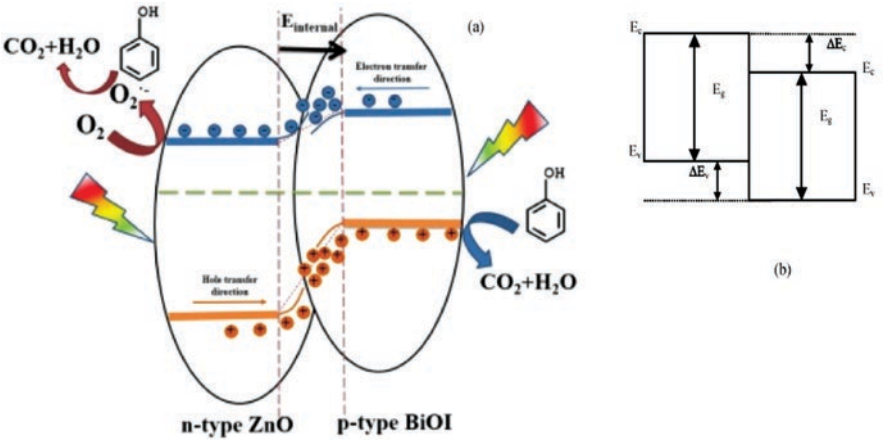

Fig. 12 (**a**) Photocatalytic mechanism scheme for separation and transfer of carriers under simulated solar light irradiated based on BiOI/ZnO photocatalyst. The red and blue lines represent the different reaction courses. (For interpretation of the references to color in this figure legend, the reader is referred to the web version of this article.) (Reproduced from Jiang et al. 2017 [172]). (**b**) Type II heterojunction with redox potential energy of CB (Ec) and VB (Ev) (Reproduced from Ani et al. 2018 [72])

the photocatalytic properties of these materials [72, 168–170]. Three types of heterojunctions that can be formed are type I, type II, and type III [72, 171] as shown in Figs. 9, 10, and 11. Type I heterojunction is displayed in Fig. 11.

A type II heterojunction involves the movement of electrons from CB which is more positive to a CB which is less negative, while the holes move from VB which is more positive to a less positive VB. The formation of type II heterojunction is shown in Fig. 12.

However, in type III heterojunction, electrons from the less negative CB move and recombine with the less positive VB holes, leaving behind holes and electrons with strong oxidation and reduction potential [72, 169]. This movement of charge carriers in the opposite direction helps in improving the effective e^-/h^+ pair

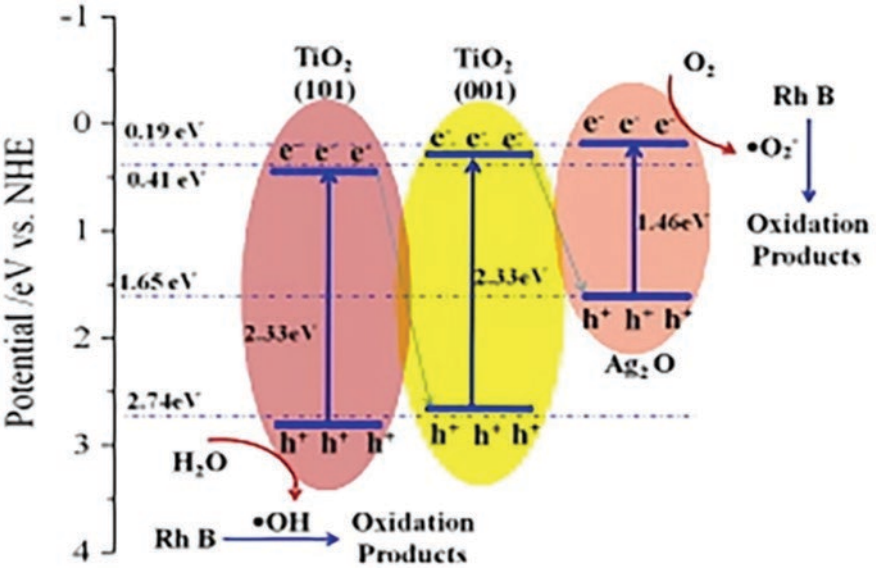

Fig. 13 Photocatalytic mechanism of Ag_2O-0.13-TiO_2 (Reproduced from Li et al. 2017 [173])

separation and hence enhances the photocatalytic performance of photocatalyst. This effective charge separation and improved photocatalytic performance along with better durability as a result of strong redox ability and wide photon response make materials with type III heterojunction the best [72, 153]. The type III heterojunction is displayed in Fig. 13.

Various composites of metal oxide-based photocatalysts have been reported for the degradation of organic pollutants. For example, a multicomponent photocatalyst was synthesized for the very first time by incorporating graphene into TiO_2 nanowires (G-Pd@TiO_2-CNW). A facile hydrothermal method and electrochemical spinning were used for the synthesis of this catalyst which possessed a porous and rough surface. The as-obtained composite was used for the degradation of 4-nitrophenol from different water samples under visible irradiation. The synergistic effect of graphene and palladium helps in enhancing the photocatalytic performance resulting in 100% degradation of 4-nitrophenol from pond water in just 30 min, while 97.2% and 80.5% degradation efficiencies were observed to reduce 4-nitrophenol from tap water and river water, respectively [174]. The mechanism of degradation of 4-nitrophenol by G-Pd@TiO_2-CNW is shown in Fig. 14.

Novel Fe_2O_3-TiO_2 nanocomposites were also prepared by using the photodeposition method and utilized for the degradation of an herbicide called 2,4-dichlorophenoxyacetic acid under both UV and visible irradiation. The as-prepared photocatalyst displayed enhanced photocatalytic performance than pristine P25 TiO_2 with maximum results for 10% Fe-TiO_2-H_2O sample. The rate constant for a composite was determined to be 2.36 min^{-1} which is 78% more than that measured with pristine P25 TiO_2. The enhanced performance was due to the

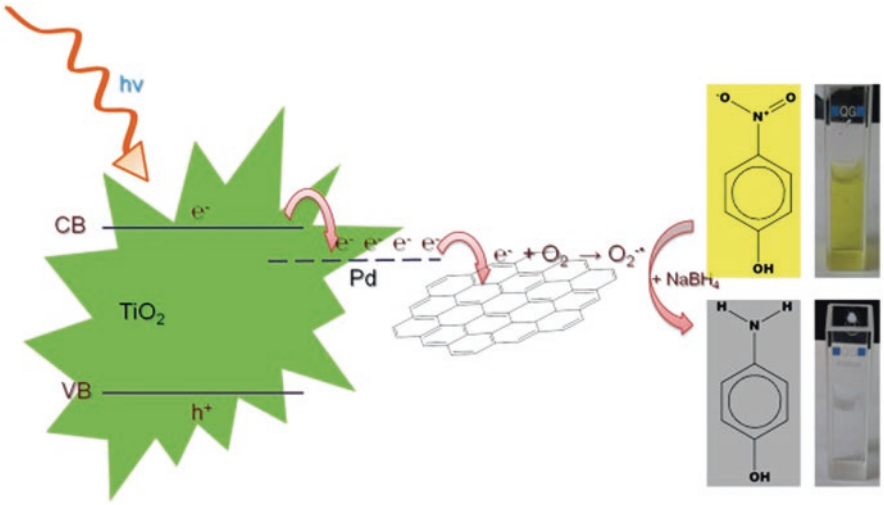

Fig. 14 Photocatalytic reduction of 4-nitrophenol by G-Pd@TiO_2-CNW (Reproduced from Lee et al. 2015 [174])

improved separation of e^-/h^+ pairs [175]. Also, MoS_2/TiO_2 photocatalyst was fabricated by hydrothermal treatment for the decomposition of paracetamol (PCM) in the presence of sunlight. The as-prepared photocatalyst was capable to decompose 40% of PCM in 25 min as compared to TiO_2 which showed decomposition of only 8% PCM. The enhanced photocatalytic performance was due to the effective charge separation inTiO_2/MoS_2 composite and the increased number of active sites to absorb visible light [176]. Furthermore, Liu et al. reported the synthesis of novel TiO_{2-x}/Ag_3PO_4composite with oxygen vacancies on which the visible light absorption depends. The photocatalytic activity of the as-synthesized photocatalyst was found to greatly depend upon the calcination temperature and the optimum temperature at which maximum degradation efficiency obtained was 400 °C. The degradation rate of TiO_{2-x}/Ag_3PO_4 was measured to be 95% for bisphenol A over 16 min of visible light irradiation which is more than pristine Ag_3PO_4 and TiO_2 [177]. Jiang et al. reported the synthesis of BiOI/ZnO photocatalyst by employing a simple and easy two-step hydrothermal method. The obtained photocatalyst was used for the photodegradation of phenol in the presence of solar light with degradation efficiency of 99.9% in 2 h. The composite showed enhanced photocatalytic activity than pure ZnO which degraded only 40% of phenol in 2 h [172]. Multifunctional photocatalyst film was also synthesized by integrating ZnO nanosheets, $BiVO_4$ particles, and conductive magnetic cilia through hydrothermal treatment. When visible light falls on the surface of the as-synthesized photocatalyst, it displayed the enhanced degradation rate towards the removal of RhB dye. The enhanced degradation rate is attributed to the improved charge separation and increased absorption and mass transfer. The degradation efficiency was calculated to be 100% in 120 min [178]. Three-dimensional SnO_2/α-Fe_2O_3 heterostructure was synthesized by

employing a facile hydrothermal approach. The obtained catalyst has displayed efficient removal efficiency towards the removal of methylene blue when visible light falls on the surface of the catalyst. The calculated degradation efficiency for methylene blue was found to be 98.4% in 240 min. The efficient removal of methylene blue contributed to the improved separation of photogenerated e^-/h^+ pairs [179]. Novel $WO_3/CdWO_4$ photocatalyst synthesized by hydrothermal and chemisorption method has been reported for the degradation of MB, MO, and RhB dyes under visible light. Maximum photocatalytic degradation was obtained for MB exhibiting 97% degradation in 50 min which was about 2.3 times more than that of pure WO_3 and seven times more than pure $CdWO_4$. The enhancement in the degradation efficiency was due to the increased surface area [180]. In another study, the synthesis of WO_3/TiO_2 photocatalyst synthesized by a sol-gel method and that displayed better photocatalytic efficiency than pure TiO_2 towards the degradation of pesticide called malathion was reported. Approximately 99% of malathion degraded in 120 min by using 2 wt% of WO_3 in the as-prepared catalyst. The improvement in the photocatalytic efficiency of TiO_2 after the introduction of WO_3 was due to the enhanced surface area and the formation of smaller clusters [181]. The nitrogen adsorption-desorption isotherm for the degradation of organophosphorus pesticide malathion is shown in Fig. 15.

Some other examples of composites of metal oxide photocatalysts for the removal of organic pollutants from water are displayed in Table 2.

4 Future Prospects

Photocatalysis has emerged as the most efficient and extensively used technique for wastewater treatment. This technique has shown remarkable progress with a long history for many years, and the progress is still ongoing. But its rate of progress still

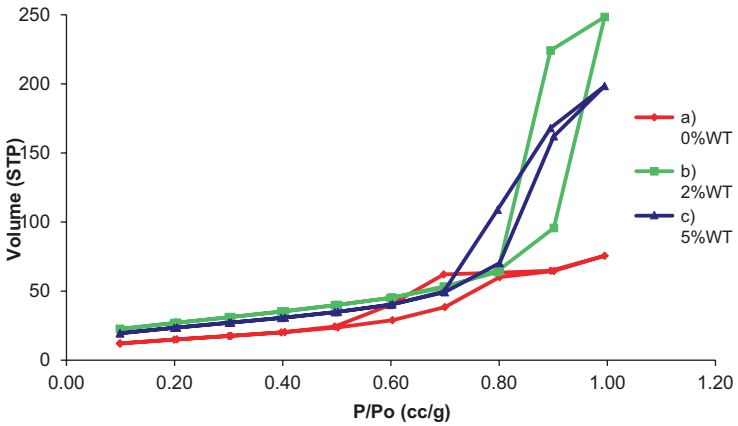

Fig. 15 Nitrogen adsorption-desorption isotherms: (**a**) 0%WT, (**b**) 2%WT, and (**c**) 5%WT (Reproduced from Ramos-Delgado et al. 2013 [181])

Table 2 List of reported metal oxide-based photocatalysts for the removal of organic pollutants from water

Pollutant	Photocatalyst	Synthesis method	Light source	Degradation efficiency (%)	Reference
2,4-Dichlorophenol	ZnO/CuO	Microwave-assisted combustion	300 W tungsten-halogen lamp	82	[182]
Rhodamine 6G	CuO/ZnO/SiNWs	Chemical precipitation	Sunlight irradiation	100	[183]
Ofloxacin	CdS/TiO_2	Hydrothermal	Visible light irradiation	86	[184]
Bisphenol A	Bi_2O_3/SnO_2	Hydrothermal	Sunlight irradiation	93.42	[185]
Rhodamine B, methylene blue, and methyl orange	$g\text{-}C_3N_4/SiO_2/SnO_2$	Sol-gel	Visible light irradiation	Methylene blue = 99.73 Methyl orange = 95.58 Rhodamine B = 95.10	[186]
Acid orange 7	$WO_3/g\text{-}C_3N_4$	Wet impregnation	Visible light irradiation	100	[187]
Methylene blue	WO_3-CuS heterojunction	Hydrothermal	300 W Xe lamp	96	[188]
Tetracycline	WO_3/Ag_3PO_4	Hydrothermal	Visible light irradiation	96	[189]
Toluene and methylene blue	CNT/TiO_2	Electrospinning and calcination	Visible irradiation	52 for toluene and 58 for methylene blue	[190]
Rhodamine B, nitrobenzene	$SWCNT/TiO_2$	Solvothermal	UV irradiation	100 both	[191]
Amoxicillin	Activated carbon-supported TiO_2 nanoparticle(s)	Ultrasonic impregnation	UV irradiation	90	[192]
Diphenhydramine	Reduced graphene oxide-TiO_2	Liquid-phase deposition	UV-Vis and visible light irradiation	>95	[193]
2,4-Dichlorophenoxy acetic acid	TiO_2-WO_3	Sol-gel	Sunlight	94.6	[194]
Tetracycline	$N\text{-}TiO_2/CaFe_2O_4$/diatomite	Sol-gel	150 W xenon lamp	91.7	[195]
Tetracycline	TiO_2/Fe_2O_3/CNT	Hydrothermal	300 W xenon lamp	89.41	[196]
Tetrabromodiphenyl ethers	TiO_2-Cu_2O film	Electrochemical deposition	300 W xenon lamp	90	[197]

Pollutant	Photocatalyst	Synthesis method	Light source	Degradation efficiency (%)	Reference
Ofloxacin	Bi_2O_3-TiO_2	Hydrothermal	70.3 K lux	92	[198]
17β-Estradiol	CdS nanorod/TiO_2 nano-belt composite	Hydrothermal	Visible irradiation	92	[199]
Ciprofloxacin	Au-CdS/TiO_2 nanowire	Molten flux	Solar light	99	[200]
Levofloxacin	Bi_2WO_6/C-dots/TiO_2	Chemical wet technique	Sunlight irradiation	99	[201]
Ciprofloxacin	Ag/Fe_2O_3/ZnO heterostructure	Precipitation method	Sunlight irradiation	76.4	[202]
2,4-Dichlorophenol	MoO_3/ZnO	Hydrothermal precipitation	55 W fluorescent lamp	99.2	[203]
Methyl orange and 4-nitrophenol	In_2O_3/ZnO	Hydrothermal	Solar light irradiation	100 for both	[204]
Methylene blue	MoS_2-ZnO heterostructure	Hydrothermal	Solar light irradiation	97	[205]
4-Chlorophenol	C/ZnO/CdS	Micro-emulsion and hydrothermal	65 W fluorescent lamp	98	[206]
Amaranth dye	Ag_2O-decorated ZnO nanorod heterostructures	Precipitation	Visible irradiation	94	[207]
Tetracycline	AgI/WO_3	Precipitation	Visible irradiation	75	[208]
Methylene blue	WO_3/g-C_3N_4	In situ liquid-phase process	Visible irradiation	97	[209]
Tetracycline	CdS/SnO_2	Hydrothermal	Visible irradiation	85	[210]
Direct blue 15	ZnO-SnO_2 nanosheets	Hydrothermal	Visible light irradiation	87	[211]
Ciprofloxacin	MoS_2-SnO_2 heterojunction anchored on expanded graphite (EG)	Hydrothermal	100 W xenon lamp	78.5	[212]

lacks to compete with the rate of deterioration of water quality. To overcome this problem, the development of widely used, economic, green, and efficient technique is necessary. Photocatalysis, although the most favorable technique for this purpose, is still unable to meet the multifarious demands of an ideal technique, as most of the studies of this technique are limited to the laboratory scale and the implementation of this technique in industries has not been achieved yet. From an industrial application point of view, the development of reactor design and an ideal photocatalytic material is a paramount task. Cost is one of the major aspects of a photocatalyst from a broad application point of view followed by environment friendliness and efficiency. These three parameters form the basis of an ideal photocatalyst. Conventional photocatalysts such as TiO_2 and ZnO have many advantages such as low cost, environment friendliness, chemical and physical stability, etc. However, they are inefficient to explore the wide spectrum of solar light. Due to their wide bandgap, they are only photoactive in the UV region which is only 5% of the solar spectrum. Thus, expensive artificial UV light is necessary for the efficient work of these catalysts, thereby increasing the cost of a photocatalyst. Therefore, visible light active materials or low bandgap materials are economic as they can be used under visible light which is nearly 48% of the solar spectrum. Recyclability is also the major aspect associated with the cost of the catalyst by ensuring their reuse. In this context, several supporting materials were reported to be used to immobilize the catalyst such as concrete, quartz, inert surface, etc. But this will lead to a decrease in the efficiency of the catalyst, hence reducing the efficiency of the operation. Thus, for the practical reuse of the material, a good support possessing specific features such as chemical stability, photochemically inert, good adsorption capability, nontoxicity, low cost, and availability in abundance is required. Another important aspect of an ideal catalyst is its toxicity. Most of the photocatalyst can convert the pollutants to mineralized products, but some of them produce intermediates that are toxic to the environment. Thus, the identification of these toxic intermediates is an imperative task, but only a few studies have focused on their identification. Therefore, extensive research is necessary to develop a prominent number of ecotoxicological tests or kits. The efficiency of the catalyst is also an important part of an ideal catalyst. Till now, various composite materials have been developed to enhance the efficiency of the catalyst, but they were still not capable to achieve up to the mark results. Nowadays, the focus of most of the researchers relies on combining photocatalysis with other wastewater treatment methods such as biological treatment, activated sludge process, ozonation, etc. which gives more efficient results. The photocatalytic efficiency not only depends upon the properties of a catalyst but also depends upon other parameters such as atmospheric conditions, properties of effluent, and the properties of a reactor. Therefore, these parameters should be optimized during the degradation of pollutants to achieve excellent efficiency. In conclusion, it is suggested that future studies should be focused on designing photocatalytic materials having good recyclability, efficiency, low cost, and environmental friendliness. Additionally, to extend the application of photocatalysis on a large scale, i.e., in industries, the focus should also be towards designing a reactor that is reliable, cost-effective, and environmentally friendly.

Acknowledgments The authors are highly grateful to Panjab University Chandigarh and A.C. Joshi Library, P.U. Chandigarh, for providing the online resources for writing this book chapter in the pandemic crisis. The authors also gratefully acknowledge the MHRD. Govt. of India's, TEQIP-III grant (2017–2020) and RUSA grant of Panjab University Chandigarh.

References

1. Mara DD (2003) Water, sanitation and hygiene for the health of developing nations. Public Health 117(6):452–456
2. Moore M, Gould P, Keary BS (2003) Global urbanization and impact on health. Int J Hyg Environ Health 206(4–5):269–278
3. World Health Organization (2018) Water sanitation hygiene. WHO global water, sanitation and hygiene annual report. https://www.who.int/water_sanitation_health/publications/global-water-sanitation-and-hygiene-annual-report-2018/en/
4. World Health Organization (2015) Progress on sanitation and drinking water. Update and MDG assessment. WHO, Geneva. https://www.unicef.org/publications/index_82419.html
5. UNICEF (2006) UNICEF, human development report. Children and water, sanitation and hygiene: the evidence. UNICEF, New York, NY. http://hdr.undp.org/en/content/children-and-water-sanitation-and-hygiene-evidence
6. United Nations, Department of Economics and Social Affairs, Population Division (2019) World Population Prospects 2019: highlights. ST/ESA/SER. A/423
7. Geissen V, Mol H, Klumpp E, Umlauf G, Nadal M, Ploega M, Zee SEATM, Ritsema CJ (2015) Emerging pollutants in the environment: a challenge for water resource management. Int Soil Water Conserv Res 3(1):57–65
8. UNESCO WWAP (2003) Water for people, water for life: 3rd world water forum in Kyoto, Japan. http://www.unesco.org/new/en/naturalsciences/environment/water/wwap/wwdr/wwdr1-2003/
9. Saxena R, Saxena M, Lochab A (2020) Recent progress in nanomaterials for adsorptive removal of organic contaminants from wastewater. Chem Select 5(1):335–353
10. Szabo E, Vajda K, Vereb G, Dombi A, Mogyorosi K, Abraham I, Majer M (2011) Removal of organic pollutants in model water and thermal wastewater using clay minerals. J Environ Sci Health A Tox Hazard Subst Environ Eng 46(12):1346–1356
11. Karpinska J, Kotowska U (2019) Removal of organic pollution in the water environment. Water 11(10):2017
12. Bhomick PC, Supong A, Sinha D (2017) Organic pollutants in water and its remediation using biowaste activated carbon as greener adsorbent. Int J Hydro 1(3):91–92
13. Vie JC, Taylor CH, Stuart SN (eds) (2009) Wildlife in a changing world – an analysis of the 2008 IUCN red list of threatened species. IUCN, Gland, Switzerland, p 180
14. Gutierreza AM, Dziublaa TD, Hilt JZ (2017) Recent advances on iron oxide magnetic nanoparticles as sorbents of organic pollutants in water and wastewater treatment. Rev Environ Health 32(1–2):111–117
15. Donde OO (2017) Wastewater management techniques: a review of advancement on the appropriate wastewater treatment principles for sustainability. Environ Manag Sustain Dev 6(1):10137
16. Rajasulochana P, Preethy V (2016) Comparison on efficiency of various techniques in treatment of waste and sewage water – a comprehensive review. Resour Eff Technol 2(4):175–184
17. Koe WS, Lee JW, Chong WC (2020) An overview of photocatalytic degradation: photocatalysts, mechanisms, and development of photocatalytic membrane. Environ Sci Pollut Res 27:2522–2565

18. Wankhade AV, Gaikwad GS, Dhonde MG, Khaty NT, Thakare SR (2013) Removal of organic pollutant from water by heterogenous photocatalysis: a review. Res J Chem Environ 17(1):84
19. Li Y, Chen F, He R, Wang Y, Tang N (2019) Semiconductor photocatalysis for water purification. Nanoscale Mater Water Purif 2019:689–705
20. Herrmann JM, Disdier J, Pichat P, Malato S, Blanco J (1998) TiO_2-based solar photocatalytic detoxification of water containing organic pollutants. Case studies of 2,4-dichlorophenoxyaceticacid (2,4-D) and of benzofuran. Appl Catal B Environ 17(1–2):15–23
21. Dong H, Zeng G, Tang L, Fan C, Zhang C, He X, He Y (2015) An overview on limitations of TiO_2-based particles for photocatalytic degradation of organic pollutants and the corresponding countermeasures. Water Res 79:128–146
22. Chakraborty S, Farida JJ, Simon R, Kasthuri S (2020) Averrhoa carambola fruit extract assisted green synthesis of ZnO nanoparticles for the photodegradation of congo red dye. Surf Interfaces 19:100488
23. Heidari Z, Alizadeh R, Ebadi A, Oturan N, Oturan MA (2020) Efficient photocatalytic degradation of furosemide by a novel sonoprecipited ZnO over ion exchanged clinoptilolite nanorods. Sep Purif Technol 242:116800
24. Sharma S, Basu S (2020) Highly reusable visible light active hierarchical porous WO_3/SiO_2 monolith in centimeter length scale for enhanced photocatalytic degradation of toxic pollutants. Sep Purif Technol 231:115916
25. Hitam CNC, Jalil AA (2020) A review on exploration of Fe_2O_3 photocatalyst towards degradation of dyes and organic contaminants. J Environ Manag 258:110050
26. Hojamberdiev M, Czech B, Goktaş AC, Yubuta K, Kadirova ZC (2020) SnO_2@ZnS photocatalyst with enhanced photocatalytic activity for the degradation of selected pharmaceuticals and personal care products in model wastewater. J Alloys Compd 827:154339
27. Mohanta D, Ahmaruzzaman M (2020) Biogenic synthesis of SnO_2 quantum dots encapsulated carbon nanoflakes: an efficient integrated photocatalytic adsorbent for the removal of bisphenol A from aqueous solution. J Alloys Compd 828:154093
28. Djurisic AB, Leung YH, Ng AMC (2014) Strategies for improving the efficiency of semiconductor metal oxide photocatalysis. Mater Horiz 1:400–410
29. Lu F, Astruc D (2020) Nanocatalysts and other nanomaterials for water remediation from organic pollutants. Coord Chem Rev 408:213180
30. Basavarajappa PS, Patil SB, Ganganagappa N, Reddy KR (2020) Recent progress in metal-doped TiO_2, non-metal doped/codoped TiO_2 and TiO_2 nanostructured hybrids for enhanced photocatalysis. Int J Hydrog Energy 45(13):7764–7778
31. Rani A, Reddy R, Sharma U, Mukherjee P, Mishra P, Kuila A, Sim LC, Saravanan P (2018) A review on the progress of nanostructure materials for energy harnessing and environmental remediation. J Nanostruct Chem 8:255–291
32. Ren Z, Guo Y, Liu CH, Gao PX (2013) Hierarchically nanostructured materials for sustainable environmental applications. Front Chem 1:18
33. Khairy M, Zakaria W (2014) Effect of metal-doping of TiO2 nanoparticles on their photocatalytic activities toward removal of organic dyes. Egypt J Pet 23(4):419–426
34. Tan YN, Wong CL, Mohamed AR (2011) An overview on the photocatalytic activity of nano-doped-TiO_2 in the degradation of organic pollutants. ISRN Mater Sci 2011:261219
35. Zhao C, Zhou Y, Ridder DJD, Zhai J, Wei Y (2014) Advantages of TiO_2/5A composite catalyst for photocatalytic degradation of antibiotic oxytetracycline in aqueous solution: comparison between TiO_2 and TiO_2/5A composite system. Chem Eng J 248:280–289
36. Guo Y, Wang P, Qian J, Hou J, Ao Y, Wang C (2018) Construction of a composite photocatalyst with significantly enhanced photocatalytic performance through combination of homojunction with hetero-junction. Cat Sci Technol 8:486–498
37. Xiao J, Xie Y, Cao H (2015) Organic pollutants removal in wastewater by heterogeneous photocatalytic ozonation. Chemosphere 121:1–17

38. Iwuozor KO (2019) Prospects and challenges of using coagulation-flocculation method in the treatment of effluents. Adv J Chem A 2(2):105–127
39. Fang F, Qiao LL, Ni BJ, Cao JS, Yu HQ (2017) Quantitative evaluation on the characteristics of activated sludge granules and flocs using a fuzzy entropy-based approach. Sci Rep 7:42910
40. Al-Abri M, Al-Ghafri B, Bora T, Dobretsov S, Dutta J, Castelletto S, Rosa L, Boretti A (2019) Chlorination disadvantages and alternative routes for biofouling control in reverse osmosis desalination. NPJ Clean Water 2:2
41. Yalcinkaya F, Boyraz E, Maryska J, Kucerova K (2020) A review on membrane technology and chemical surface modification for the oily wastewater treatment. Materials (Basel) 13(2):493
42. Boddu VM, Paul T, Page MA, Byl C, Ward L, Ruan J (2016) Gray water recycle: effect of pretreatment technologies on low pressure reverse osmosis treatment. J Environ Chem Eng 4(4):4435–4443
43. Esmaeili H, Foroutan R (2015) Investigation into ion exchange and adsorption methods for removing heavy metals from aqueous solutions. Int J Biol Pharm Allied Sci 4:620–629
44. Zhang M, Dong H, Zhao L, Wang DX, Meng D (2019) A review on Fenton process for organic wastewater treatment based on optimization perspective. Sci Total Environ 670:110–121
45. Khulbe KC, Matsuura T (2018) Removal of heavy metals and pollutants by membrane adsorption techniques. Appl Water Sci 8:19
46. Li X, Xie J, Jiang C, Yu J, Zhang P (2018) Review on design and evaluation of environmental photocatalysts. Front Environ Sci Eng 12(5):14
47. Melchionna M, Fornasiero P (2020) Updates on the roadmap for photocatalysis. ACS Catal 10:5493–5501
48. Fujishima A, Honda K (1972) Electrochemical photolysis of water at a semiconductor electrode. Nature 238:37–38
49. Saravanan R, Gracia F, Stephen A (2017) Basic principles, mechanism, and challenges of photocatalysis. In: Khan M, Pradhan D, Sohn Y (eds) Nanocomposites for visible light-induced photocatalysis. Springer series on polymer and composite materials. Springer, Cham
50. Zhang F, Wang X, Liu H, Liu C, Wan Y, Long Y, Cai Z (2019) Recent advances and applications of semiconductor photocatalytic technology. Appl Sci 9:2489
51. Khan MM, Adil SF, Mayouf AA (2015) Metal oxides as photocatalysts. J Saudi Chem Soc 19(5):462–464
52. Ahmed SN, Haider W (2018) Heterogeneous photocatalysis and its potential applications in water and wastewater treatment: a review. Nanotechnology 29:342001
53. Zhu D, Zhou Q (2019) Action and mechanism of semiconductor photocatalysis on degradation of organic pollutants in water treatment: a review. Environ Nanotechnol Monit Manag 12:100255
54. Chong M, Jin B, Chow CWK, Saint C (2010) Recent developments in photocatalytic water treatment technology: a review. Water Res 44(10):2997–3027
55. Ibhadon AO, Fitzpatrick P (2013) Heterogeneous photocatalysis: recent advances and applications. Catalysts 3(1):189–218
56. Al-Rasheed R, Arabia S (2005) Water treatment by heterogeneous photocatalysis an overview. Chemistry 2005:15
57. Shaheen K, Suo H, Arshad T, Shah Z, Khan SA, Khan SB, Khan MN, Liu M, Ma L, Cui J, Ji YT, Wang Y (2020) Metal oxides nanomaterials for the photocatalytic mineralization of toxic water wastes under solar light illumination. J Water Process Eng 34:101138
58. Hoffmann MR, Martin ST, Choi W, Bahnemann DW (1995) Environmental applications of semiconductor photocatalysis. Chem Rev 95(1):69–96
59. Nakata K, Fujishima A (2012) TiO_2 photocatalysis: design and applications. J Photochem Photobiol C Photochem Rev 13(3):169–189
60. Shayegan Z, Lee CS, Haghighat F (2018) TiO_2 photocatalyst for removal of volatile organic compounds in gas phase – a review. Chem Eng J 334:2408–2439

61. Khalilova HK, Hasanova SA, Aliyev FG (2018) Photocatalytic removal of organic pollutants from industrial wastewater using TiO_2 catalyst. J Environ Prot 9(6):691–698
62. Ong CB, Ng LY, Mohammad AW (2018) A review of ZnO nanoparticles as solar photocatalysts: synthesis, mechanisms and applications. Renew Sust Energ Rev 81(1):536–551
63. Qiu R, Zhang D, Mo Y, Song L, Brewer E, Huang X, Xiong Y (2008) Photocatalytic activity of polymer-modified ZnO under visible light irradiation. J Hazard Mater 156(1–3):80–85
64. Karthikeyan C, Arunachalam P, Ramachandran K, Mayouf AMA, Karuppuchamy S (2020) Recent advances in semiconductor metal oxides with enhanced methods for solar photocatalytic applications. J Alloys Compd 828:154281
65. Pinho L, Mosquera MJ (2013) Photocatalytic activity of TiO_2–SiO_2 nanocomposites applied to buildings: influence of particle size and loading. Appl Catal B Environ 134-135:205–221
66. Frank SN, Bard AJ (1977) Heterogeneous photocatalytic oxidation of cyanide and sulfite in aqueous solutions at semiconductor powders. J Phys Chem 81(15):1484–1488
67. Inoue T, Fujishima A, Konishi S, Honda K (1979) Photoelectrocatalytic reduction of carbon dioxide in aqueous suspensions of semiconductor powders. Nature 277:637–638
68. Horikoshi S, Serpone N (2020) Can the photocatalyst TiO_2 be incorporated into a wastewater treatment method? Background and prospects. Catal Today 340:334–346
69. Shvadchina YO, Vakulenko VF, Levitskaya EE, Goncharuk VV (2012) Photocatalytic destruction of anionic SAS with oxygen and hydrogen peroxide in the TiO_2 suspension. J Water Chem Technol 34:218–226
70. Teh CM, Mohamed AR (2011) Roles of titanium dioxide and ion-doped titanium dioxide on photocatalytic degradation of organic pollutants (phenolic compounds and dyes) in aqueous solutions: a review. J Alloys Compd 509(5):1648–1660
71. Hernandez-Alonso MD, Fresno F, Suarez S, Coronado JM (2009) Development of alternative photocatalysts to TiO_2: challenges and opportunities. Energy Environ Sci 2:1231–1257
72. Ani IJ, Akpan UG, Olutoye MA, Hameed BH (2018) Photocatalytic degradation of pollutants in petroleum refinery wastewater by TiO_2- and ZnO-based photocatalysts: recent development. J Clean Prod 205:930–954
73. Al-Mamun MR, Kader S, Islam MS, Khan MZH (2019) Photocatalytic activity improvement and application of UV-TiO_2 photocatalysis in textile wastewater treatment: a review. J Environ Chem Eng 7(5):103248
74. Zhang J, Zhou P, Liu J, Yu J (2014) New understanding of the difference of photocatalytic activity among anatase, rutile and brookite TiO_2. Phys Chem Chem Phys 16:20382–20386
75. Fisher K, Gawel A, Rosen D, Krause M, Latif AA, Griebel J, Prager A, Schulze A (2017) Low-temperature of anatase/rutile/brookite TiO_2 nanoparticles on a polymer membrane for photocatalysis. Catalysts 7(7):209
76. Guimaraes RR, Parussulo ALA, Araki K (2016) Impact of nanoparticles preparation method on the synergic effect in anatase/rutile mixtures. Electrochim Acta 222:378–1386
77. Hussain M, Ceccarelli R, Marchisio DL, Fino D, Russo N, Geobaldo F (2010) Synthesis, characterization, and photocatalytic application of novel TiO_2 nanoparticles. Chem Eng J 157(1):45–51
78. Chen H, Nanayakkara CE, Grassian VH (2012) Titanium dioxide photocatalysis in atmospheric chemistry. Chem Rev 112(11):5919–5948
79. Pfeifer V, Erhart P, Li S, Rachut K, Morasch J, Brotz J, Reckers P, Mayer T, Ruhle S, Zaban A, Sero IM, Bisquert J, Jaegermann W, Klein A (2013) Energy band alignment between anatase and rutile TiO_2. J Phys Chem Lett 4(23):4182–4187
80. Hussain M, Russo N, Saracco G (2011) Photocatalytic abatement of VOCs by novel optimized TiO_2 nanoparticles. Chem Eng J 166(1):138–149
81. Wang C, Wu T (2015) TiO_2 nanoparticles with efficient photocatalytic activity towards gaseous benzene degradation. Ceram Int 41(2):2836–2839
82. Colombo DP Jr, Bowman RM (1996) Chemical physics of nanostructured semiconductors. J Phys Chem 100:18445

83. Gaya UI, Abdullah AH (2008) Heterogeneous photocatalytic degradation of organic contaminants over titanium dioxide: a review of fundamentals, progress and problems. J Photochem Photobiol C Photochem Rev 9(1):1–12
84. Chen C, Lu C, Chung Y, Jan J (2007) UV light induced photodegradation of malachite green on TiO_2 nanoparticles. J Hazard Mater 141(3):520–528
85. Faisal M, Tariq MA, Muneer M (2007) Photocatalysed degradation of two selected dyes in UV-irradiated aqueous suspensions of titania. J Dyes Pigments 72:233–239
86. Yang L, Yu LE, Ray MB (2008) Degradation of paracetamol in aqueous solutions by TiO2 photocatalysis. Water Res 42:3480–3488
87. Ohko Y, Ando I, Niwa C, Tatsuma T, Yamamura T, Nakashima T, Kubota Y, Fujishima A (2001) Degradation of bisphenol A in water by TiO_2 photocatalyst. Environ Sci Technol 35:2365–2368
88. Kumar SG, Rao KSRK (2015) Zinc oxide based photocatalysis: tailoring surface-bulk structure and related interfacial charge carrier dynamics for better environmental applications. RSC Adv 5:3306–3351
89. Look DC, Reynolds DC, Sizelove JR, Jones RL, Litton CW, Cantwell G, Harsch WC (1998) Electrical properties of bulk ZnO. Solid State Commun 105(6):399–401
90. Chandiran AK, Jalebi MA, Nazeeruddin MK, Gratzel M (2014) Analysis of electron transfer properties of ZnO and TiO_2 photoanodes for dye-sensitized solar cells. ACS Nano 8(3):2261–2268
91. Kamat PV, Bedja I, Hotchandani S (1994) Photoinduced charge transfer between carbon and semiconductor clusters. One-electron reduction of C60 in colloidal TiO_2 semiconductor suspensions. J Phys Chem 98(37):9137–9142
92. Daneshvar N, Salari D, Khataee AR (2004) Photocatalytic degradation of azo dye acid red 14 in water on ZnO as an alternative catalyst to TiO_2. J Photochem Photobiol A Chem 162(2–3):317–322
93. Fenoll J, Ruiz E, Hellín P, Flores P, Navarro S (2011) Heterogeneous photocatalytic oxidation of cyprodinil and fludioxonil in leaching water under solar irradiation. Chemosphere 85(8):262–1268
94. Sakthivel S, Neppolian B, Shankar MV, Arabindoo B, Palanichamy M, Murugesan V (2003) Solar photocatalytic degradation of azo dye: comparison of photocatalytic efficiency of ZnO and TiO_2. Sol Energy Mater Sol Cells 77(1):65–82
95. Shafaei A, Nikazar M, Arami M (2010) Photocatalytic degradation of terephthalic acid using titania and zinc oxide photocatalysts: comparative study. Desalination 252(1–3):8–16
96. Han J, Liu Y, Singhal N, Wang L, Gao W (2012) Comparative photocatalytic degradation of estrone in water by ZnO and TiO_2 under artificial UVA and solar irradiation. Chem Eng J 213:150–162
97. Movahedi M, Mahjoub AR, Janitabar-Darzi S (2009) Photodegradation of Congo red in aqueous solution on ZnO as an alternative catalyst to TiO_2. JICS 6:570–577
98. Mohabansi NP, Patil VB, Yenkie N (2011) A comparative study on photo degradation of methylene blue dye effluent by advanced oxidation process by using TiO_2/ZnO photo catalyst. Rasayan J Chem 4(4):814–819
99. Kamat PV, Huehn R, Nicolaescu R (2002) A "sense and shoot" approach for photocatalytic degradation of organic contaminants in water. J Phys Chem B 106(4):788–794
100. Quintana M, Edvinsson T, Hagfeldt A, Boschloo G (2007) Comparison of dye-sensitized ZnO and TiO_2 solar cells: studies of charge transport and carrier lifetime. J Phys Chem C 111(2):1035–1041
101. Muruganandham M, Zhang Y, Suri R, Lee GJ, Chen PK, Hsieh SH, Sillanpyaa M, Wu JJ (2015) Environmental applications of ZnO materials. J Nanosci Nanotechnol 15(9):6900–6913
102. Tian C, Zhang Q, Wu A, Jiang M, Liang Z, Jiang B, Fu H (2012) Cost-effective large-scale synthesis of ZnO photocatalyst with excellent performance for dye photodegradation. Chem Commun 48:2858–2860

103. Poulios I, Kositzi M, Kouras A (1998) Photocatalytic decomposition of triclopyr over aqueous semiconductor suspensions. J Photochem Photobiol A Chem 115(2):175–183
104. Hariharan C (2006) Photocatalytic degradation of organic contaminants in water by ZnO nanoparticles: revisited. Appl Catal A Gen 304:55–61
105. Colon G, Hidalgo MC, Navio JA, Melian EP, Diaz OG, Rodriguez JMD (2008) Highly photoactive ZnO by amine capping-assisted hydrothermal treatment. Appl Catal B Environ 83:30–38
106. Liao Y, Xie C, Liu Y, Huang Q (2013) Metal oxide-based photocatalysis: fundamentals and prospects for application. J Alloys Compd 550:190–197
107. Daneshvar N, Aber S, Dorraji MSS, Khataee AR, Rasoulifard MH (2007) Photocatalytic degradation of the insecticide diazinon in the presence of prepared nanocrystalline ZnO powders under irradiation of UV-C light. Sep Purif Technol 58(1):91–98
108. El-Kemary M, El-Shamy H, El-Mehasseb I (2010) Photocatalytic degradation of ciprofloxacin drug in water using ZnO nanoparticles. J Lumin 130:2327–2331
109. Anju SG, Yesodharan S, Yesodharan EP (2012) Zinc oxide mediated sonophotocatalytic degradation of phenol in water. Chem Eng J 189–190:84–93
110. Chen X, Wu Z, Liu D, Gao Z (2017) Preparation of ZnO photocatalyst for the efficient and rapid photocatalytic degradation of azo dyes. Nanoscale Res Lett 12:143–152
111. Zhang Z, Hossain MF, Takahashi T (2010) Self-assembled hematite (α-Fe2O3) nanotube arrays for photoelectrocatalytic degradation of azo dye under simulated solar light irradiation. Appl Catal B 95(3–4):423–429
112. Cong Y, Chen M, Xu T, Zhang Y, Wang Q (2014) Tantalum and aluminum co-doped iron oxide as a robust photocatalyst for water oxidation. Appl Catal B 147:733–740
113. Pradhan GK, Sahu N, Parida KM (2013) Fabrication of S, N co-doped α-Fe_2O_3 nanostructures: effect of doping, OH radical formation, surface area, [110] plane and particle size on the photocatalytic active. RSC Adv 3:7912–7920
114. Wu W, Jiang C, Roy VAL (2015) Recent progress in magnetic iron oxide–semiconductor composite nanomaterials as promising photocatalysts. Nanoscale 7:38–58
115. Liu X, Chen K, Shim JJ, Huang J (2015) Facile synthesis of porous Fe_2O_3 nanorods and their photocatalytic properties. J Saudi Chem Soc 19:479–484
116. Lu AH, Salabas EL, Schuth F (2007) Magnetic nanoparticles: synthesis, protection, functionalization, and application. Angew Chem Int Ed 46:1222–1244
117. Laurent S, Forge D, Port M, Roch A, Robic C, Elst LV, Muller RN (2008) Magnetic iron oxide nanoparticles: synthesis, stabilization, vectorization, physicochemical characterizations, and biological applications. Chem Rev 108:2064–2110
118. Gondal MA, Sayeed MN, Yamani ZH, Al-Arfaj AR (2009) Efficient removal of phenol from water using Fe_2O_3 semiconductor catalyst under UV laser irradiation. J Environ Sci Health A Tox Hazard Subst Environ Eng 44(5):515–521
119. Shao P, Ren Z, Tian J, Gao S, Luo X, Shi W, Yan B, Li J, Cui F (2017) Silica hydrogel-mediated dissolution-recrystallization strategy for synthesis of ultrathin α-Fe_2O_3nanosheets with highly exposed (1 1 0) facets: a superior photocatalyst for degradation of bisphenol S. Chem Eng J 323:64–73
120. Dou M, Persson C (2013) Comparative study of rutile and anatase SnO_2 and TiO_2: band-edge structures, dielectric functions, and polaron effects. J Appl Phys 113(2013):083703
121. Abe R, Higashi M, Sayama K, Abe Y, Sugihara H (2006) Photocatalytic activity of R_3MO_7 and $R_2Ti_2O_7$ (R = Y, Gd, La; M = Nb, Ta) for water splitting into H_2 and O_2. J Phys Chem B 110:2219–2226
122. Madelung O, Rossler U, Schulz M (1998) Tin dioxide (SnO_2) crystal structure, lattice parameters, thermal expansion non-tetrahedrally bonded elements and binary compounds I. Springer, Berlin, pp 1–2
123. Mistry BV, Avasthi DK, Joshi US (2016) Tuning of optical and electrical properties of wide band gap Fe:SnO_2/Li:NiO p–n junctions using 80 MeV oxygen ion beam. Appl Phys A Mater Sci Process 122:1024

124. Zhang G, Xie C, Zhang S, Zhang S, Xiong Y (2014) Defect chemistry of the metal cation defects in the p-and n-doped SnO_2 nanocrystalline films. J Phys Chem C 118:18097–18109
125. Sanal KC, Jayaraj MK (2013) Growth and characterization of tin oxide thin films and fabrication of transparent p-SnO/n-ZnO p–n hetero junction. Mater Sci Eng B 178:816–821
126. Zulfiqar Y, Yang J, Wang W, Ye Z, Ye JL (2016) Structural and optical properties of (Zn, Co) co-doped SnO_2 nano particles. J Mater Sci Mater Electron 27:12119–12127
127. Paramarta V, Taufik A, Munisa L, Saleh R (2017) Sono- and photocatalytic activities of SnO_2 nanoparticles for degradation of cationic and anionic dyes. AIP Conf Proc 1788:030125
128. Yashas SR, Shivaraju HP, Thinley T, Pushparaj KS, Maleki A, Shahmoradi B (2020) Facile synthesis of SnO_2 2D nanoflakes for ultrasound-assisted photodegradation of tetracycline hydrochloride. Int J Environ Sci Technol 17:2593–2604
129. Viet PV, Thi CM, Hieu LV (2016) The high photocatalytic activity of SnO_2 nanoparticles synthesized by hydrothermal method. Photochem Photobiol 87(2):267–274
130. Tahir MB, Ali S, Rizwan M (2019) A review on remediation of harmful dyes through visible light-driven WO_3 photocatalytic nanomaterials. Int J Environ Sci Technol 16:4975–4988
131. Aslam I, Cao C, Khan WS, Tanveer M, Abid M, Idrees F, Riasat R, Tahir M, Butta FK, Alia Z (2014) Synthesis of three-dimensional WO_3 octahedra: characterization, optical and efficient photocatalytic properties. RSC Adv 4:37914–37920
132. Huang J, Xiao L, Yang X (2013) WO_3 nanoplates, Hierarchical flower-like assemblies and their photocatalytic properties. Mater Res Bull 48:2782–2785
133. Nguyen TT, Nam S-N, Son J, Oh J (2019) Tungsten trioxide (WO_3)-assisted photocatalytic degradation of amoxicillin by simulated solar irradiation. Sci Rep 9:9349
134. Jeevanandam J, Barhoum A, Chan YS, Dufresne A, Danquah MK (2018) Review on nanoparticles and nanostructured materials: history, sources, toxicity and regulations. Beilstein J Nanotechnol 9:1050–1074
135. Yu X, Hu Y, Zhou L, Cao F, Yang Y, Liang T, He J (2011) Research progress of nanostructured materials for heterogeneous catalysis. Curr Nanosci 7(4):11
136. Xu Z, Meng X (2009) Size effects of nanocrystalline TiO_2 on As(V) and As(III) adsorption and As(III) photooxidation. J Hazard Mater 168:747
137. Falk GS, Borlaf M, Lopez-Munoz MJ, Farinas JC, Neto JBR, Moreno R (2018) Microwave-assisted synthesis of TiO_2 nanoparticles: photocatalytic activity of powders and thin film. J Nanopart Res 20:23
138. Liu Z, Zhang X, Nishimoto S, Murakami T, Fujishima A (2008) Efficient photocatalytic degradation of gaseous acetaldehyde by highly ordered TiO_2 nanotube arrays. Environ Sci Technol 42:8547
139. Kansal SK, Sood S, Umar A, Mehta SK (2013) Photocatalytic degradation of Eriochrome Black T dye using well-crystalline anatase TiO2 nanoparticles. J Alloys Compd 51:392–397
140. Fang K, Wang Z, Zhang M, Wang A, Meng Z, Feng J (2013) Gelatin-assisted hydrothermal synthesis of single crystalline zinc oxide nanostars and their photocatalytic properties. J Colloid Interface Sci 402:68–74
141. Kansal SK, Lamba R, Mehta SK, Umar A (2013) Photocatalytic degradation of Alizarin Red S using simply synthesized ZnO nanoparticles. Mater Lett 106:385–389
142. Deng J, Liu J, Dai H, Wang W (2018) Preparation of α-Fe_2O_3 nanowires through electrospinning and their Ag_3PO_4 heterojunction composites with enhanced visible light photocatalytic activity. Ferroelectrics 528:58–65
143. Wu S, Cao H, Yin S, Liu X, Zhang X (2009) Amino acid-assisted hydrothermal synthesis and photocatalysis of SnO_2 nanocrystals. J Phys Chem C 113:17893–17898
144. Asahi R, Morikawa T, Irie H, Ohwaki T (2014) Nitrogen-doped titanium dioxide as visible-light-sensitive photocatalyst: designs, developments, and prospects. Chem Rev 114(19):9824–9852
145. Huang J, Guo X, Wang B, Li L, Zhao M, Dong L, Liu X, Huang Y (2015) Synthesis and photocatalytic activity of Mo-doped TiO_2 nanoparticles. J Spectrosc 2015:681850

146. Qiu L, Luo X (2018) ZIF-8 derived Ag-doped ZnO photocatalyst with enhanced photocatalytic activity. RSC Adv 8:4890–4894
147. Bousslama W, Elhouichet H, Ferid M (2017) Enhanced photocatalytic activity of Fe doped ZnO nanocrystals under sunlight irradiation. Optik 134:88–98
148. Arshad M, Ehtisham-ul-Haque S, Bilal M, Ahmad N, Ahmad A, Abbas M, Nisar J, Khan MI, Nazir A, Ghaffar A, Iqbal M (2020) Synthesis and characterization of Zn doped WO_3 nanoparticles: photocatalytic, antifungal and antibacterial activities evaluation. Mater Res Express 7:015407
149. Wang Y, Chan K, Li X, So S (2006) Electrochemical degradation of 4-chlorophenol at nickel–antimony doped tin oxide electrode. Chemosphere 65:1087–1093
150. Chen L, Li F, Ni B, Xu J, Fu Z, Lu Y (2012) Enhanced visible photocatalytic activity of hybrid Pt/α-Fe_2O_3 nanorods. RSC Adv 2:10057–10063
151. Xie W, Li R, Xu Q (2018) Enhanced photocatalytic activity of Se-doped TiO_2 under visible light irradiation. Sci Rep 8:1–10
152. Maragatha J, Rani C, Rajendran S, Karuppuchamy S (2017) Microwave synthesis of nitrogen doped Ti_4O_7 for photocatalytic applications. Phys E 93:78–82
153. Kubacka A, Munoz-Batista MJ, Ferrer M, Fernandez-Garcia M (2018) Er-W codoping of TiO_2-anatase: structural and electronic characterization and disinfection capability under UV-vis, and near-IR excitation. Appl Catal B Environ 228:113–129
154. Zhong JB, Li JZ, He XY, Zeng J, Lu Y, Hu W, Lin K (2012) Improved photocatalytic performance of Pd-doped ZnO. Curr Appl Phys 12:998–1001
155. Kaur A, Gupta G, Ibhadon AO, Salunke DB, Sinha ASK, Kansal SK (2018) A Facile synthesis of silver modified ZnO nanoplates for efficient removal of ofloxacin drug in aqueous phase under solar irradiation. J Environ Chem Eng 6(3):3621–3630
156. Qiu Y, Yang M, Fan H, Xu Y, Shao Y, Yang X, Yang S (2013) Synthesis and characterization of nitrogen doped ZnO tetrapods and application in photocatalytic degradation of organic pollutants under visible light. Mater Lett 99:105–107
157. Fadavieslam MR (2016) Effect of Sb doping on the structural, electrical, and optical properties of SnO_2 thin films prepared through spray pyrolysis. J Mater Sci Mater Electron 27:4943–4950
158. Kuvarega AT, Krause RWM, Mamba BB (2012) Multiwalled carbon nanotubes decorated with nitrogen, palladium co-doped TiO_2 (MWCNT/N, Pd co-doped TiO_2) for visible light photocatalytic degradation of eosin yellow in water. J Nanopart Res 2012:776–779
159. Chelli VR, Golder AK (2017) Bimetal doping on TiO_2 for photocatalytic water treatment: a green route. Eur Water 58:53–60
160. Yan H, Kochuveedu ST, Quan LN, Lee SS, Kim DH (2013) Enhanced photocatalytic activity of C, F-codoped TiO_2 loaded with AgCl. J Alloys Comp 560:20–26
161. Benhebal H, Chaib M, Malengreaux C, Leonard A, Lambert SD, Leonard A, Crine M, Heinrichs B (2014) Visible-light photo-activity of alkali metal doped ZnO. J Taiwan Inst Chem Eng 45(1):249–253
162. Lu J, Wang H, Peng D, Chen T, Dong S, Chang Y (2016) Synthesis and properties of Au/ZnO nanorods as a plasmonic photocatalyst. Phys E Low Dimens Syst Nanostruct 78:41
163. Lamba R, Umar A, Mehta SK, Kansal SK (2015) ZnO doped SnO_2 nanoparticles heterojunction photo-catalyst for environmental remediation. J Alloys Compd 653:327–333
164. Wu C (2014) Facile one-step synthesis of N-doped ZnO micropolyhedrons for efficient photocatalytic degradation of formaldehyde under visible-light irradiation. Appl Surf Sci 319:237
165. Yousef A, Barakat NAM, Amna T, Unnithan AR, Al-Deyab SS, Yong Kim H (2012) Influence of CdO-doping on the photoluminescence properties of ZnO nanofibers: effective visible light photocatalyst for waste water treatment. J Lumin 132(7):1668–1677
166. Sin J, Lam S, Lee K, Mohamed AR (2015) Preparation of cerium-doped ZnO hierarchical micro/nanospheres with enhanced photocatalytic performance for phenol degradation under visible light. J Mol Catal A Chem 409:1–10

167. Wang H, Cai Y, Zhou J, Fang J, Yang Y (2017) Crystallization-mediated amorphous CuxO (x = 1, 2)/crystalline CuI p–p type heterojunctions with visible light enhanced and ultraviolet light restrained photocatalytic dye degradation performance. Appl Surf Sci 402:31–40
168. Lan H, Li L, An X, Liu F, Chen C, Liu H (2017) Microstructure of carbon nitride affecting synergetic photocatalytic activity : hydrogen bonds vs. structural defects. Appl Catal B Environ 204:49–57
169. Wang J, Xia Y, Zhao H, Wang G, Xiang L, Xu J, Komarneni S (2017) Oxygen defects-mediated Z-scheme charge separation in g-C_3N_4/ZnO photocatalysts for enhanced visible-light degradation of 4-chlorophenol and hydrogen evolution. Appl Catal B Environ 206:406–416
170. Yao J, Chen H, Jiang F, Jiao Z, Jin M (2017) Titanium dioxide and cadmium sulfide co-sensitized graphitic carbon nitride nanosheets composite photocatalysts with superior performance in phenol degradation under visible-light irradiation. J Colloid Interface Sci 490:154–162
171. Heng H, Gan Q, Meng P, Liu X (2017) The visible-light-driven type III heterojunction$H_3PW_{12}O_{40}/TiO_2$-In_2S_3: a photocatalysis composite with enhanced photocatalytic activity. J Alloy Comp 696:51–59
172. Jiang J, Wang H, Chen X, Li S, Xie T, Wang D, Lin Y (2017) Enhanced photocatalytic degradation of phenol and photogenerated charges transfer property over BiOI-loaded ZnO composites. J Colloid Interface Sci 494:130–138
173. Li M, Liu H, Liu T, Qin Y (2017) Design of a novel dual Z-scheme photocatalytic system composited of Ag_2O modified Ti^{3+} self doped TiO_2 nanocrystals with individual exposed (001) and (101) facets. Mater Charact 124:136–144
174. Lee H, Sai-Anand G, Komathi S, Gopalan AI, Kang SW, Lee KP (2015) Efficient visible-light-driven photocatalytic degradation of nitrophenol by using graphene-encapsulated TiO_2 nanowires. J Hazard Mater 283:400–409
175. Moniz SJA, Shevlin SA, An X, Guo ZX, Tang J (2014) Fe_2O_3-TiO_2 nanocomposites for enhanced charge separation and photocatalytic activity. Chem Eur J 20:15571–15579
176. Kumar N, Bhadwal AS, Mizaikoff B, Singh S, Kranz C (2019) Electrochemical detection and photocatalytic performance of MoS_2/TiO_2 nanocomposite against pharmaceutical contaminant: paracetamol. Sens Bio-Sens Res 24:100288
177. Liu J, Xie F, Li R, Li T, Jia Z, Wang Y, Wang Y, Zhang X, Fan C (2019) TiO_2-x/Ag_3PO_4 photocatalyst: oxygen vacancy dependent visible light photocatalytic performance and BPA degradative pathway. Mater Sci Semicond Process 97:1–10
178. Construction (2017) Construction of ZnO nanosheet arrays within $BiVO_4$ particles on a conductive magnetically driven cilia film with enhanced visible photocatalytic activity. J Alloys Compd 690:953
179. Zhang S, Li J, Niu H, Xu W, Xu J, Hu W, Wang X (2013) Visible-light photocatalytic degradation of methylene blue using SnO_2/α-Fe_2O_3 hierarchical nanoheterostructures. ChemPlusChem 78(2):192–199
180. Aslam I, Cao C, Tanveer M, Farooq MH, Khan WS, Tahir M, Idrees F, Khalid S (2015) A novel Z-scheme $WO_3/CdWO_4$ photocatalyst with enhanced visible-light photocatalytic activity for the degradation of organic pollutants. RSC Adv 5:6019–6026
181. Ramos-Delgado NA, Gracia-Pinilla MA, Maya-Trevino L, Hinojosa-Reyes L, Guzman-Mar JL, Hernandez-Ramirez A (2013) Solar photocatalytic activity of TiO_2 modified with WO_3 on the degradation of an organophosphorus pesticide. J Hazard Mater 263(1):36–44
182. Sherly ED, Vijaya JJ, Kennedy LJ (2015) Visible-light-induced photocatalytic performances of ZnO–CuO nanocomposites for degradation of 2,4-dichlorophenol. Chin J Catal 36:1263
183. Feng Q, Li SY, Ma WH, He X, Zou YX (2017) Hydrothermal synthesis of flower-like CuO/ZnO/SiNWs photocatalyst for degradation of r6g under visible light irradiation. Key Eng Mater 727:847
184. Kaur A, Umar A, Anderson WA, Kansal SK (2018) Facile synthesis of CdS/TiO_2 nanocomposite and their catalytic activity for ofloxacin degradation under visible illumination. J Photochem Photobiol A 360:34–43

185. Chu L, Zhang J, Wu Z, Wang C, Sun Y, Dong S, Sun J (2020) Solar-driven photocatalytic removal of organic pollutants over direct Z-scheme coral-branch shape Bi_2O_3/SnO_2 composites. Mater Charact 159:110036
186. Peng L, Zheng R, Feng D, Yu H, Dong X (2020) Synthesis of eco-friendly porous g-C_3N_4/SiO_2/SnO_2 composite with excellent visible-light responsive photocatalysis. Arab J Chem 13(2):4275–4285
187. Priya A, Senthil RA, Selvi A, Arunachalam P, Kumar CKS, Madhavan J, Boddula R, Pothu R, Al-Mayouf AM (2020) A study of photocatalytic and photoelectrochemical activity of as-synthesized WO_3/g-C_3N_4 composite photocatalysts for AO_7 degradation. Mater Sci Energy Technol 3:43–50
188. Liu Y, Li M, Zhang Q, Qin P, Wang X, He G, Li L (2020) One-step synthesis of a WO_3-CuS nanosheet heterojunction with enhanced photocatalytic performance for methylene blue degradation and Cr(VI) reduction. Chem Technol Biotechnol 95(3):665–674
189. Pudukudy M, Shan S, Miao Y, Gu B, Jia Q (2020) WO_3 nanocrystals decorated Ag_3PO_4 tetrapods as an efficient visible-light responsive Z-scheme photocatalyst for the enhanced degradation of tetracycline in aqueous medium. Colloids Surf A Physicochem Eng Asp 589:124457
190. Wongaree M, Chiarakorn S, Chuangchote S, Sagawa T (2016) Photocatalytic performance of electrospun CNT/TiO_2 nanofibers in a simulated air purifier under visible light irradiation. Environ Sci Pollut Res 23:21395–21406
191. Zhou W, Pan K, Qu Y, Sun F, Tian C, Ren Z, Fu H (2010) Photodegradation of organic contamination in wastewaters by bonding TiO_2/single-walled carbon nanotube composites with enhanced photocatalytic activity. Chemosphere 81(5):555–561
192. Basha S, Barr C, Keane D, Nolan K, Morrissey A, Oelgemoller M, Tobin JM (2011) On the adsorption/photodegradation of amoxicillin in aqueous solutions by an integrated photocatalytic adsorbent (IPCA): experimental studies and kinetics analysis. Photochem Photobiol Sci 10:1014–1022
193. Pastrana-Martinez LM, Morales-Torres S, Likodimos V, Figueiredo JL, Faria JL, Falaras P, Silva AMT (2012) Advanced nanostructured photocatalysts based on reduced graphene oxide-TiO_2 composites for degradation of diphenhydramine pharmaceutical and methyl orange dye. Appl Catal B Environ 2012:123–124
194. Macias-Tamez R, Villanueva-Rodriguez M, Ramos-Delgado NA, Maya-Trevino L, Hernandez-Ramirez A (2017) Comparative study of the photocatalytic degradation of the herbicide 2,4-D Using WO_3/TiO_2 and Fe_2O_3/TiO_2 as catalysts. Water Air Soil Pollut 228:379
195. Chen Y, Wu Q, Wang J, Song Y (2019) The fabrication of magnetic recyclable nitrogen-doped titanium dioxide/calcium ferrite/diatomite heterojunction nanocomposite for improved visible-light-driven degradation of tetracycline. J Chem Technol Biotechnol 94:2702–2712
196. Lu C, Guan W, Zhang G, Ye L, Zhou Y, Zhang X (2013) TiO_2 /Fe_2O_3/CNTs magnetic photocatalyst: a fast and convenient synthesis and visible-light-driven photocatalytic degradation of tetracycline. Micro Nano Lett 8:749–752
197. Hu Z, Wang X, Dong H, Li S, Li X, Li L (2017) Efficient photocatalytic degradation of tetrabromodiphenyl ethers and simultaneous hydrogen production by TiO_2-Cu_2O composite films in N_2 atmosphere: influencing factors, kinetics and mechanism. J Hazard Mater 340:1–15
198. Sood S, Mehta SK, Sinha ASK, Kansal SK (2016) Bi_2O_3/TiO_2 heterostructures: synthesis, characterization and their application in solar light mediated photocatalyzed degradation of an antibiotic, ofloxacin. Chem Eng J 290:45–52
199. Luo L, Long J, Zhao S, Dai J, Ma L, Wang H, Xia L, Shu L, Jiang F (2019) Effective visible-light-driven photocatalytic degradation of 17α-ethynylestradiol by crosslinked CdS nanorod/TiO_2 (B) nano-belt composite. Process Saf Environ Prot 130:77–851
200. Kandi D, Behera A, Martha S, Naik B, Parida KM (2019) Quantum confinement chemistry of CdS QDs plus hot electron of Au over TiO_2 nanowire protruding to be encouraging photo-

catalyst towards nitrophenol conversion and ciprofloxacin degradation. J Environ Chem Eng 7:102821
201. Sharma S, Ibhadon AO, Francesconi MG, Mehta SK, Elumalai S, Kansal SK, Umar A, Baskoutas S (2020) Bi_2WO_6/C-Dots/TiO_2: a novel z-scheme photocatalyst for the degradation of fluoroquinolone levofloxacin from aqueous medium. Nano 10(5):910
202. Kaur A, Anderson WA, Tanvir S, Kansal SK (2019) Solar light active silver/iron oxide/zinc oxide heterostructure for photodegradation of ciprofloxacin, transformation products and antibacterial activity. J Colloid Interface Sci 557:236–253
203. Lam S, Sin J, Abdullah AZ, Mohamed AR (2013) Investigation on visible-light photocatalytic degradation of 2,4-dichlorophenoxyacetic acid in the presence of MoO_3/ZnO nanorod composites. J Mol Catal A Chem 370:123
204. Liu H, Zhai H, Hu C, Yang J, Liu Z (2017) Hydrothermal synthesis of In_2O_3 nanoparticles hybrid twins hexagonal disk ZnO heterostructures for enhanced photocatalytic activities and stability. Nanoscale Res Lett 12:466
205. Ritika M, Kaur A, Umar SK, Mehta S, Singh SK, Kansal HF, Alothman OY (2018) Rapid solar-light driven superior photocatalytic degradation of methylene blue using MoS_2-ZnO heterostructure nanorods photocatalyst. Materials (Basel) 11(11):2254
206. Lavand AB, Malghe YS (2015) Visible light photocatalytic degradation of 4-chlorophenol using C/ZnO/CdS nanocomposites. J Saudi Chem Soc 19(5):471–478
207. Lamba R, Umar A, Mehta SK, Kansal SK (2017) Enhanced visible light driven photocatalytic application of Ag2O decorated ZnO nanorods heterostructures. Sep Purif Technol 183:341–349
208. Wang T, Quan W, Jiang D, Chen L, Li D, Meng S, Chen M (2016) Synthesis of redox-mediator-free direct Z-scheme AgI/WO_3 nanocomposite photocatalysts for the degradation of tetracycline with enhanced photocatalytic activity. Chem Eng J 300:280–290
209. Liu X, Jin A, Jia Y, Xia T, Deng C, Zhu M, Chen C, Chen X (2017) Synergy of adsorption and visible-light photocatalytic degradation of methylene blue by a bifunctional Z-scheme heterojunction of WO_3/g-C_3N_4. Appl Surf Sci 405:359–371
210. Zhang L, Niu CG, Liang C, Wen X, Huang D, Guo H, Zhao X, Zeng G (2018) One-step in situ synthesis of CdS/SnO_2 heterostructure with excellent photocatalytic performance for Cr(VI) reduction and tetracycline degradation. Chem Eng J 352:863–875
211. Lamba R, Umar A, Mehta SK, Kansal SK (2015) Well-crystalline porous ZnO–SnO_2 nanosheets: an effective visible-light driven photocatalyst and highly sensitive smart sensor material. Talanta 131:490–498
212. Umukoro EH, Kumar N, Ngila JC, Arotiba OA (2018) Expanded graphite supported p-n MoS_2-SnO_2 heterojunction nanocomposite electrode for enhanced photo-electrocatalytic degradation of a pharmaceutical pollutant. J Electroanal Chem 827:193–203